NASA CR-135387
PWA-5569-12

NASA

(NASA-CR-135387) DEVELOPMENT OF A PLASMA SPRAYED CERAMIC GAS PATH SEAL FOR HIGH PRESSURE TURBINE APPLICATION Final Report, 9 Jun. 1977 - 9 Jan. 1978 (Pratt and Whitney Aircraft Group) 86 p HC A05/MF A01 CSCL 21E G3/07 N78-24141 Unclas 20800

DEVELOPMENT OF A PLASMA SPRAYED CERAMIC GAS PATH SEAL FOR HIGH PRESSURE TURBINE APPLICATION FINAL REPORT

by L. T. Shiembob

Pratt & Whitney Aircraft Group
Commercial Products Division
United Technologies Corporation

Prepared for
National Aeronautics and Space Administration

NASA-Lewis Research Center
Contract NAS3-20623

1. Report No.	2. Government Accession No.	3. Recipient's Catalog No.
NASA CR-135387		

4. Title and Subtitle	5. Report Date
Development of a Plasma Sprayed Ceramic Gas Path Seal For High Pressure Turbine Applications	May 1978
	6. Performing Organization Code
7. Author(s)	8. Performing Organization Report No.
L. T. Shiembob	PWA-5569-12
	10. Work Unit No.
9. Performing Organization Name and Address Pratt & Whitney Aircraft Group Commercial Products Division United Technologies Corporation East Hartford, Connecticut 06108	11. Contract or Grant No. NAS3-20623
12. Sponsoring Agency Name and Address Propulsion Laboratory U. S. Army R&T Labs (AVRADCOM) Lewis Research Center Cleveland, Ohio 44135	13. Type of Report and Period Covered Contractor Report 6/9/77 – 1/9/78
	14. Sponsoring Agency Code

15. Supplementary Notes

Project Manager, Dr. Robert C. Bill
NASA Lewis Research Center
Cleveland, Ohio 44135

16. Abstract

Development of the plasma sprayed graded, layered ZrO_2/CoCrAlY seal system for gas turbine engine blade tip seal applications up to 1589°K (2400°F) surface temperature initiated under NASA contracts NAS3-18565 and NAS3-19759 was continued. The effect of changing ZrO_2/CoCrAlY ratios in the intermediate layers on thermal stresses was evaluated analytically with the goal of identifying the materials combinations which would minimize thermal stresses in the seal system. Three methods of inducing compressive residual stresses in the sprayed seal materials to offset tensile thermal stresses were analyzed. The most promising method, thermal prestraining, was selected based upon potential, feasibility and complexity considerations. The plasma spray equipment was modified to heat, control and monitor the substrate temperature during spraying. Specimens were fabricated and experimentally evaluated to 1) substantiate the capability of the thermal prestrain method to develop compressive residual stresses in the sprayed structure and 2) to define the effect of spraying on a heated substrate on abradability, erosion and thermal shock characteristics of the seal system. Thermal stress analysis, including residual stresses and material properties variations, was performed and correlated with thermal shock test results. Seal system performance was assessed and recommendations for further development were made.

Results of the analysis performed indicates the 85/15 and 40/60 ZrO_2/CoCrAlY ratios used in contract NAS3-19759 were approximately optimum with regards to minimizing sprayed seal system thermal stresses. The capability of thermal prestraining the substrate during spraying of the seal system to induce compressive residual stresses in the sprayed materials was substantiated. Experimental results indicated spraying on a heated substrate had negligible effects on abradability characteristics of the seal system. However, thermal shock testing and subsequent thermal stress analysis indicated that the presence of compressive residual stresses caused a new failure mode with rapid spallation, not observed in specimens sprayed without compressive residual stresses. Also, the supplemental heating used to produce the compressive residual stresses was found to significantly affect material properties. (continued on page ii)

17. Key Words (Suggested by Author(s))	18. Distribution Statement
Seal, Abradable Seal, Turbine Seal, Blade Tip Seal, Gas Path Seal, Plasma sprayed (continued on page ii)	

19. Security Classif. (of this report)	20. Security Classif. (of this page)	21. No. of Pages	22. Price*
Unclassified	Unclassified		

* For sale by the National Technical Information Service, Springfield, Virginia 22161

NASA-C-168 (Rev. 10-75)

16. **Abstract (Cont'd)**

The seal system, sprayed without supplemental heating of the substrate, performed much better during thermal fatigue testing than any previous configurations. One hundred simulated engine thermal cycles were completed before inspection revealed initiation of slight radial cracks. Five hundred cycles were completed successfully without spallation. The seal system sprayed on heated substrates developed severe laminar cracks during the initial heatup cycle. This performance correlates well with analytical results. Analysis indicated significant potential for residual stress management to reduce thermal stresses but additional development is required to realize the maximum benefit.

17. **Key Words (Cont'd)**

Seal, Ceramic
Seal, High Temperature
Zirconia
Abradability
Erosion
Elastic Modulus
Thermal Conductivity
Thermal Expansion
Thermal Shock
Thermal Stress
Rupture Modulus
Ultimate Strength
Residual Stress
Prestress
Properties, Materials
Properties, Physical
Properties, Mechanical

FOREWORD

This report describes the work accomplished under contract NAS3-20623 by Commercial Products Division of Pratt & Whitney Aircraft (P&WA) Group, United Technologies Corporation for the Lewis Research Center of the National Aeronautics and Space Administration. The technical effort was initiated on 9 June 1977 and completed on 9 January 1978.

Dr. Robert C. Bill of the National Aeronautics and Space Administration (NASA) was the Project Manager and Mr. Leonard W. Schopen of the NASA Lewis Research Center was the Contracting Officer.

Mr. Lawrence T. Shiembob was the Program Manager for Pratt & Whitney Aircraft.

Appreciation is extended to the following P&WA personnel for their assistance: Oscar L. Stewart, Senior Experimental Engineer, for overall program assistance; G. Scott Bosshart, Analytical Engineer, for assistance with thermal stress analysis; Martin J. Reiner, Assistant Materials Project Engineer, and Arnold S. Grot, Materials Engineer, for assistance in determining materials properties and metallurgical analyses.

TABLE OF CONTENTS

LIST OF ILLUSTRATIONS

LIST OF ILLUSTRATIONS (Cont'd)

LIST OF ILLUSTRATIONS (Cont'd)

LIST OF TABLES

1.0 SUMMARY AND CONCLUSIONS

1.1 SUMMARY OF RESULTS

Analysis indicated little benefit by changing the ZrO_2/CoCrAlY ratios of the intermediate zirconia-metal (ZrO_2/CoCrAlY) layers of the plasma sprayed ZrO_2/CoCrAlY turbine blade tip seal configuration developed under contract NAS3-19759. ZrO_2 layer stresses could be reduced slightly but maximum stresses could not be reduced below the measured minimum material strength. Intermediate layer stress reduction was not an objective of this analysis because stresses in these layers are within their respective measured strength.

The relative potential, feasibility and complexity of mechanical and thermal prestraining of the metal substrate and of post spray annealing to induce compressive residual stresses in the plasma sprayed ZrO_2/CoCrAlY seal system were evaluated. Thermal prestraining of the metal substrate was selected as the most promising method. The plasma spray equipment and fixturing was modified to provide capability of heating, controlling and monitoring the metal substrate temperature during spraying of the seal system.

Analysis indicated that the magnitude of induced compressive residual stresses in the sprayed seal system was sensitive to the stiffness, as well as to the cross sectional area, of the metal substrate. Consequently, the seal configuration was modified to use a 0.254 cm (0.10 in) thick platform instead of the 0.127 cm (0.05 in) platform thickness used in the final NAS3-19759 seal configuration. This was the only change made to the seal system configuration. Powder ratios and layer thicknesses were the same as the NAS3-19759 configuration.

Test specimens of this modified configuration were sprayed with and without supplemental heating of the metal substrates for experimental evaluation of the effect of residual stress management on seal system performance. Abradability, erosion and thermal shock rig tests were conducted on each set of specimens.

Abradability resistance characteristics of the specimens sprayed or heated substrates were essentially the same as demonstrated by NAS3-19759 specimens (sprayed without supplemental heating).

Thermal shock test results indicate very promising performance for the seal sprayed without supplemental heating of the substrate (baseline seal system). The baseline seal system completed 100 cycles without noticeable crack initiation and 500 thermal shock cycles without spallation — much better performance than exhibited by the final NAS3-19759 seal after 100 thermal cycles. Three seals sprayed on heated substrates [922°K (1200°) seal system] exhibited severe laminar cracking or delamination after the initial acceleration cycle.

Residual strains were measured in specimens sprayed with and without supplemental heating of the metal substrates and were used to calculate stress free temperature distributions in the seal systems. These stress free temperature distributions were used in a two-dimensional finite element plane stress computer program to incorporate residual stress effects with calculated thermal stresses.

Moduli of elasticity and rupture, strain to failure, thermal expansivity and thermal conductivity were determined for each seal layer material sprayed on heated metal substrates. This data indicated significant variations from properties determined for seal layer materials sprayed without supplemental substrate heating under NAS3-19759.

Thermal stresses were calculated in the seal system for a typical gas turbine engine idle to sea level takeoff thermal cycle and for measured rig test cycle conditions. Stresses calculated for actual rig test conditions using both residual strain and properties data measured for the 922°K (1200°F) seal system correlated well with experimental results, i.e., fractures occurred in the locations and under thermal conditions indicated by the analytical results. Analysis of the baseline seal system could not be completed because of uncertainty of the residual stress distribution in this configuration.

1.2 CONCLUSIONS

Performance of the plasma sprayed ZrO_2/CoCrAlY seal systems evaluated in this program may be summarized as follows:

1. Thermal shock resistance of the baseline system (without supplemental heating) sprayed onto a 0.254 cm (0.100 in) substrate rather than onto a 0.127 cm substrate, as under NAS3-19759, demonstrated a marked improvement over previous sprayed systems.

2. Analysis indicated the potential benefit of thermal management of residual stress on the thermal stress in the sprayed ceramic system. Compressive residual stresses induced in the system by spraying on a heated substrate did reduce operating stresses in the central portion of the seal. However, the effect near the edges was small and maximum stress still exceeded the strength in the ZrO_2 and 85/15 ZrO_2/CoCrAlY layers.

3. Thermal shock resistance of the seal system sprayed on 922°K (1200°F) metal substrates was unsatisfactory. Analysis correlated well with test results.

4. Abradability characteristics were not significantly affected by spraying on heated substrates.

The concept of using compressive residual stresses to reduce operating thermal stresses in the sprayed seal system still appears to be viable except for edge effects. The application of this concept must, therefore, be tailored to optimize the residual stress level and distribution.

Material properties, especially of the ZrO_2/CoCrAlY intermediate layers, appear to change significantly by spraying on heated metal substrates. These property variations significantly affect the temperature and stress distributions in the seal system. More complete definition of sprayed seal system material properties as functions of temperature and of the thermal condition of the metal substrate during spraying is required to obtain more valid analytical results.

Microstructural examination of the plasma sprayed materials indicates powder particles tend to deposit in layers of interlocking flattened irregular shaped disks. This results in a non-homogeneous microstructure and could indicate anisotropic properties within these materials which should be investigated as a possible contributing factor in laminar cracking at the edge of the specimens.

2.0 RECOMMENDATIONS

Measurement of residual stresses in the baseline ZrO_2/CoCrAlY seal system should be repeated to permit correlation of analytical and experimental test results and to quantify the effect of spraying on a heated substrate on residual and operating stresses.

Improvement of the residual stress distribution combined with seal system configuration considerations such as metal substrate stiffness should be explored. Reduction of the tensile stresses near the edge similar to the stress reductions calculated in the central portion of the seal system may be possible by changing the residual stress distribution or the seal segment geometry, or some combination of both. Variations of individual layer stress free temperatures, circumferential and axial dimensions and substrate thickness and/or stiffness should be analyzed.

More complete definition of sprayed materials properties is needed to more accurately predict performance of the ZrO_2/CoCrAlY seal system. Elastic and rupture modulii in the radial direction should be measured to investigate the anisotropic nature of system properties. Tensile and compressive modulii of elasticity and rupture as functions of both operating temperature and metal substrate temperature during spraying should be more completely defined. Thermal conductivity of intermediate layer materials should be measured instead of estimated from composite seal system measurements. Variability of properties and microstructure due to thermal aging and due to substrate temperature during spraying should also be investigated.

The assumption that spraying on a modified metal substrate configuration for residual stress determination would not significantly affect the stress free temperature distribution should be substantiated. Stress free temperature distributions for specimens sprayed on standard substrate configurations which are modified to reduce stiffness subsequent to spraying should be determined for comparison with specimens sprayed on premodified substrates.

A sharp discontinuity of the thermal conditions in the seal system occurs at layer interfaces due to interruption of the spray process to change materials. Interfacial strengths have been assumed equal to the weakest of the two materials. Verification of this assumption or quantification of the actual bond properties should be pursued.

3.0 INTRODUCTION

3.1 BACKGROUND

The program to develop a plasma sprayed yttria stabilized ceramic (zirconia)-metal (CoCrAlY) seal system initiated under contract NAS3-18565 and continued under contract NAS3-19759 produced encouraging results. A configuration composed of a zirconia top layer and intermediate mixed layers of zirconia and CoCrAlY demonstrated promising abradability and erosion resistance capability at operating surface temperatures of 1589°K (2400°F). Of paramount importance, however, was the capability of the system to withstand the thermal shock and fatigue environment expected in an engine. Seal specimens subjected to thermal fatigue rig tests produced cracks predominantly in the ZrO_2 layer, confirming analytical results, but did not spall. Efforts to minimize cyclic thermal stresses by optimization of layer thicknesses resulted in a promising improvement in that the extent of cracking was reduced substantially.

Analyses performed under NAS3-18565 and NAS3-19759 did not account for residual stresses. Measured room temperature residual stresses approached the tensile strength of the zirconia layer and are believed to have contributed to thermal cracking in the zirconia layer. The analytical programs used for these contracts have subsequently been modified under P&WA funded programs to permit incorporation of residual stresses.

3.2 PROGRAM OVERVIEW

This program was a continuation of the effort conducted under NAS3-18565 and NAS3-19759 to develop a graded, layered plasma sprayed zirconia-CoCrAlY turbine blade tip seal system capable of operation up to 1589°K (2400°F). The objective of this program was to reduce cyclic thermal stresses to an acceptable level to maintain the integrity of the seal system without compromising abradability and erosion resistance. Two methods of accomplishing this were investigated:

1. Optimization of the zirconia - metal mixture of the intermediate layers, and
2. Prestraining the metal substrate during fabrication processing to produce compressive residual stresses in the ceramic seal system.

The effect of zirconia-metal ratio variations in the intermediate layers on thermal cyclic stresses were analytically investigated. The results of this analysis would serve as a basis for selection of material ratios with desirable property combinations to minimize cyclic thermal stresses.

Material properties data obtained under NAS3-19759 were used for estimating properties of materials with different zirconia-metal ratios.

Methods of reducing tensile residual stresses in the sprayed ceramic seal system were evaluated. The goal of this effort was the generation of compressive residual stresses in the sprayed system to counteract tensile cyclic thermal stresses. The most promising method was experimentally evaluated.

A complete seal system incorporating the selected optimized materials fabricated with and without the selected residual stress management method were experimentally evaluated. Abradability, erosion resistance and thermal fatigue rig tests were conducted. Residual stresses and material properties for each seal layer were measured.

The experimental test results were evaluated and the capability of the seal system relative to program objectives was assessed. Abradability, erosion resistance and other data such as hardness and microstructure was compared with NAS3-19759 data to obtain an indication of the repeatability of seal system performance. Recommendations for further development were formulated.

4.0 TECHNICAL PROGRAM

4.1 CONFIGURATION OPTIMIZATION

Analysis under NAS3-19759 to evaluate the effect of layer thicknesses in the plasma sprayed zirconia-metal seal system on thermal stresses resulted in the generation of a configuration which improved the thermal shock resistance of the seal system.(1) Experimental results correlated with analysis which predicted significant reduction in thermal cyclic stresses although the reduction was not sufficient to reduce maximum principal stresses in the ZrO_2 layer to less than its measured strength. Because of the lack of appropriate analytical program provision at the time, the effect of residual stresses, which may have contributed to the cracking in this seal configuration, was not accounted for in these analyses.

The effect of changing materials in the mixed ZrO_2-CoCrAlY layers between the ZrO_2 surface layer and the Mar-M-509 metal substrate to further reduce cyclic thermal stresses in the selected seal configuration was analytically investigated. Material properties obtained under NAS3-19759 for ZrO_2 and 85/15, 70/30 and 40/60 ZrO_2/CoCrAlY (spray powder weight ratios) plasma sprayed materials were crossplotted, as shown in Figures 1 through 7, to estimate the properties of the revised layer material. Properties were updated from data obtained from NAS3-19759, literature and/or from other P&WA programs.

The configuration which resulted from the NAS3-19759 layer optimization was composed of layer thicknesses of 0.229 cm (0.090 in) for the ZrO_2, 0.076 cm (0.030 in) each for the 85/15 and 40/60 ZrO_2/CoCrAlY intermediate layers and 0.127 cm (0.050 in) for the Mar-M-509 metal substrate platform. This configuration was selected as the baseline for this analysis to evaluate the significance of material ratios and select a configuration which offered potential to reduce thermal stresses. Seal geometry and layer thicknesses were held constant. Since previous studies had indicated that stresses in the circumferential plane were greater than those in the axial section, this study considered the circumferential section as shown in Figure 8. Circumferential stresses near the free surfaces and the interfaces between seal material layers at the center of the seal and approximately 0.48 cm (0.19 in) from the ends of the seal were analyzed. These locations were selected since experience has shown that stresses in these locations usually approach minimum or maximum values. Figure 8 shows the seal configuration and the location of reported stresses and temperatures.

Temperatures and stresses were calculated using the same two-dimensional finite element computer programs used for NAS3-19759 analyses. A one-dimensional temperature gradient radially through the seal system was assumed. Boundary conditions on the ceramic surface and the metal substrate surface were assumed the same for each configuration variation studied and internal temperature distributions were computed. These temperature distributions were then used in the plane stress program to calculate the two dimensional stress distribution in each configuration. A nominal JT9D-70 engine thermal cycle, the same as used in analysis under the previous contract, was used in this evaluation. Four thermal cycle

(1) Shiembob, L. T., Development of a Plasma Sprayed Ceramic Gas Path Seal For High Pressure Turbine Applications, NASA CR-135183 (PWA-5521), p. 37.

points were considered: idle, six seconds after initiation of acceleration, SLTO and 12 seconds after initiation of deceleration. However, since maximum stresses occur in the baseline configuration at SLTO and 6 seconds into acceleration, temperatures and stresses were calculated only at these two points. Residual stresses were assumed to be zero.

Selection of the first two configuration variations was based on a preliminary analysis of the baseline configuration which indicated that changing the 40/60 and 85/15 ZrO_2/CoCrAlY layers to 10/90 and 70/30 ZrO_2/CoCrAlY, respectively, would result in the closest possible approximation to a linear average thermal growth gradient between the ZrO_2 layer and the metal substrate for the four most significant thermal cycle points. The effect of each of these changes was analyzed independently. The third configuration variation with 10/90 and 90/10 ZrO_2/CoCrAlY layers was selected on the basis of evaluation of the first two configurations.

Calculated temperatures and stresses in the baseline configuration and the three selected configuration variations are shown in Tables I and II. This data indicates:

1. Reducing the ZrO_2/CoCrAlY ratio of layer 1 tends to:

   a. Reduce stresses in layer 1 except at the interface with layer 2 near the ends of the seal where stresses are increased slightly.

   b. Increase the maximum stresses in the ZrO_2 and No. 2 layers and in the metal substrate.

2. Reducing the ZrO_2/CoCrAlY ratio of layer 2 tends to:

   a. Increase the ZrO_2 layer stresses at the interface with layer 2.

   b. Increase stresses in layer 2.

   c. Reduce stresses in layer 1 and the metal substrate.

3. Simultaneous reduction of the ZrO_2/CoCrAlY ratio of layer 1 and increasing of the ZrO_2/CoCrAlY ratio of layer 2 tends to:

   a. Have only small effects on the ZrO_2 layer and metal substrate stresses.

   b. Increase stresses in layer 2.

   c. Reduce stresses in layer 1.

In assessing the effects of material ratio changes, stress to strength ratio as well as stress level was considered.

On the basis of this study, it was concluded:

1. Varying the ZrO_2/CoCrAlY ratio of the intermediate layers result in relatively small (~10%) changes in the ZrO_2 layer stresses. These changes are not sufficient to eliminate the possibility of thermal stress cracking of the ceramic layer.

2. Redistribution of stresses within the intermediate layers by changing their ZrO_2/CoCrAlY mixtures is possible but the potential gains are relatively small.

In view of the minimal potential gains in terms of reduced thermal stresses and the costly necessity of establishing a new data base for the new materials, it was decided not to change the baseline system configuration for this program.

4.2 PRESTRESS APPLICATION METHOD DEVELOPMENT

The potential, feasibility, complexity and risk associated with three possible methods of prestressing the metal substrate to generate compressive residual stresses in the plasma sprayed graded ZrO_2-CoCrAlY seal system were analyzed. The methods analyzed were:

1. Mechanical prestressing by bending and by uniform tensile loading equally in mutually perpendicular planes,

2. Heating of the metal substrate during spraying, and

3. Post spraying annealing.

Both substrate heating during spraying and mechanical prestressing were found to be feasible but mechanical prestressing was considered much more complex and a higher risk than thermal preheating. Post spray annealing was not considered feasible because of excessive stresses induced at the 40/60 ZrO_2/CoCrAlY layer - metal substrate interface at temperatures well below the temperature at which reasonable creep rates occur in the metal substrate.

Heating the metal substrate was selected as the most promising method to induce compressive residual stresses in the sprayed ZrO_2-CoCrAlY seal system when all factors were considered. In this method the substrate is elongated during the spray process by an external heat source. After the seal material has been deposited the external heat source is removed allowing the substrate to attempt to contract to its normal room temperature state, thereby providing a compressive load in the deposited seal system. The plasma spray equipment was modified to permit heating the metal substrates while spraying the seal system. Abradability specimens were fabricated and residual stress measurements were made to evaluate the feasibility and effectiveness of this residual stress management method.

4.2.1 Mechanical Prestressing

Two approaches to mechanically prestressing the substrate were evaluated; bending and uniform tensile stressing equally in mutually perpendicular planes. The sprayed materials were assumed to be deposited on the metal substrate while it was maintained in the prestressed state. After spraying, the prestress would be released and the substrate would react with the sprayed structure as it attempted to return to its initial state.

A flat plate model of the baseline seal configuration 0.0762 cm (0.030 in) 40/60 ZrO_2/CoCrAlY, 0.0762 cm (0.030 in) 85/15 ZrO_2/CoCrAlY, and 0.2286 cm (0.090 in) ZrO_2 layers deposited on a Mar-M-509 metal substrate, was used in this analysis. Residual stresses were assumed to be solely due to release of the prestress in the substrate after spraying. The two-dimensional plane stress finite element computer program used in NAS3-19759 analyses and material properties measured under NAS3-19759 were used to calculate the residual stresses in the seal system.

The effect of uniform tensile prestressing of the substrate on residual stress induced at the surface of the ZrO_2 layer for various substrate thicknesses is shown in Figure 9. This data indicates that the thickness of the metal substrate has a significant effect on the induced stress at the ZrO_2 surface. Compressive stresses would be induced at the ZrO_2 surface for substrate thicknesses greater than approximately 0.381 cm (0.150 in). At any point in the seal system the stress is comprised of the sum of the elongation and bending components. The elongation component is compressive throughout the sprayed system and is a function of the metal substrate cross-sectional area and prestrain. The bending component is tensile from the ZrO_2 surface to the section neutral axis and compressive on the opposite side of the neutral axis. The bending component is proportional to the amount of bending induced in the specimen and distance from the neutral axis. The relative stiffness of the sprayed system and metal substrate will determine the amount of bending for a given substrate prestrain level. This general relationship would also be true for heating (thermal prestraining) of the substrate. Therefore, this analysis indicates the necessity to use metal substrates with equivalent stiffness greater than that of a 0.381 cm (0.150 in) thick flat plate to induce compressive residual stresses by both uniform tensile prestressing and heating of the substrate. This does not mean that the minimum substrate thickness must be 0.381 cm (0.150 in) or greater. For instance, the abradability rig test specimen metal substrate has a circumferential direction stiffness equivalent to a flat plate 0.574 cm (0.226 in) thick although the maximum metal thickness is only 0.254 cm (0.100 in).

Mechanical prestressing is limited by the thickness and strength of the metal substrate. Figure 10 shows the stress induced at the ZrO_2 surface as a function of substrate thickness for maximum prestress in the metal substrate equal to 80 percent of the 0.2 percent yield strength of the substrate. Both bending and tensile prestress approaches are shown. The bending approach produces larger compressive stresses for thicknesses less than approximately 0.635 cm (0.250 in). It approaches a maximum induced compressive stress at thicknesses greater than 0.635 cm (0.250 in) while the tensile loading method will continue to induce larger compressive stresses at the ZrO_2 surface as the thickness is increased.

Although the tensile loading approach indicates the maximum potential for inducing compressive stresses in the sprayed seal system, the problems of fixturing to prestress complex substrate geometries required for engine and rig tests, i.e., short segments of a ring with integral supporting and stiffening structure on the outside diameter, would be complex and costly.

Prestressing by bending would be difficult to control precisely due to the small deflections required; 0.00254 cm (0.001 in) - 0.00381 cm (0.0015 in) for typical parts with 0.635 cm (0.250 in) thickness or equivalent stiffness. However, it is considered more feasible and less costly than tensile prestressing.

4.2.2 Substrate Heating

The effect of substrate heating on an abradability specimen during spraying was analytically evaluated. The metal substrate was assumed to be stress free at the substrate temperature and the plasma sprayed system was assumed stress free at various temperatures equal to or greater than the substrate temperature. Residual stresses calculated at the ZrO_2 surface in the center of the specimen are shown in Figure 11 as a function of substrate temperature for constant temperature differences between stress free temperatures for the sprayed materials and the substrate. This data indicates the potential to induce compressive residual stresses in the sprayed system increases as the substrate temperature is increased and decreases as the sprayed materials stress free temperature approaches the substrate temperature.

Assuming that the difference between stress free temperature of the sprayed system and the substrate is less than 333°K (600°F), Figure 11 indicates a substrate temperature of approximately 922°K (1200°F) would be needed to induce compressive stresses at the ZrO_2 surface of the magnitude of the maximum tensile thermal cyclic stresses, 4.137×10^3 N/cm^2 (6×10^3 psi) to 6.206×10^3 N/cm^2 (9×10^3 psi).

The two-dimensional plane stress computer program used for NAS3-19759 analyses was modified under a P&WA funded program to provide the capability to assign varying stress free temperatures throughout the seal system. This change allowed the program to calculate residual stress distributions and combine them with cyclic thermal stresses. Thermal growths are calculated based on the temperature difference between the local temperature and the local stress free temperature. This modified computer program was used to calculate residual stresses for this substrate heating study. For the first time in a NASA contract, thermal stress analyses included the effects of residual stresses.

Heating the substrate is the simplest, most practical method of uniformly prestraining the metal substrate in mutually perpendicular directions. It has the advantage over the mechanical prestress method that the equilibrium stress in the substrate, not the initial prestress, is limited by the yield strength and geometric configuration of the substrate material. Except for the question of the effect of substrate heating on sprayed material properties, this method of residual stress management has the maximum potential.

4.2.3 Post Spraying Annealing

The objective of the post spraying annealing is to induce compressive stresses in the sprayed seal by heating the as-sprayed seal to develop a sufficiently high tensile stress in the metal substrate at a temperature level which would result in significant creep.

To evaluate post spray annealing, stresses were calculated for isothermal heating to 811°K (1000°F), 1144°K (1600°F) and 1256°K (1800°F) and for gradient heating from 2144°K (3400°F) on the ZrO_2 surface to 1200°K (1700°F) on the substrate surface using the 0.635 cm (0.250 in) thick flat metal plate model used in the mechanical prestress analysis. Residual stresses were neglected in this analysis. Stresses in the 40/60 ZrO_2/CoCrAlY layer exceeded its rupture strength at all isothermal conditions except 811°K (1000°F). Further analysis indicated that the maximum substrate temperature compatible with the 40/60 ZrO_2/CoCrAlY rupture strength was approximately 1006°K (1350°F). At this temperature, the creep rate of the substrate at the calculated stress level is less than 2×10^{-7} %/hr, which is unacceptably low compared to the desired minimum creep rate of 1×10^{-5} %/hr. Obtaining acceptable temperature and stress combinations by gradient heating was evaluated and was found not to be feasible.

4.2.4 Residual Stress Management Method Evaluation

Heating the metal substrate was selected as the most promising residual stress management method based on 1) potential to develop the desired level of compressive residual stresses in the plasma sprayed materials, 2) minimum complexity and 3) low risk. Alternative methods of heating the metal substrate during spraying were evaluated. The most promising meth method was selected. The plasma spraying equipment was modified to permit substrates heating and maintaining the metal substrates at the desired elevated temperature and to continuously monitor the metal substrate temperature during the complete processing cycle. Specimens were fabricated to demonstrate capability of producing compressive residual stresses and to serve as a basis for selection of a processing method for subsequent complete seal system specimens for rig tests.

4.2.4.1 Plasma Spray Equipment Modifications

Both electric and gas heating were considered as methods of heating the metal substrates during spraying of the seal system. Propane gas heating was selected due to response rate, flexibility, cost and availability considerations.

Heating of the metal substrates was accomplished by six (6) propane burners equally spaced in a stationary metal ring around the outside of the spray fixture as shown in Figure 12. The burners were positioned such that the hottest part of the flame would impinge on the outside of the metal substrates when operating at maximum flows. The burners were manifolded together in groups of three and supplied from a common propane tank and pressure regulator. A needle valve in the supply line to each manifold permits separate control of each group of three burners.

The plasma spray torch was enclosed in an asbestos board box to protect it from excessive heat from the propane burners as shown in the foreground of Figure 12. Later this was reduced to wrapping with two or three layers of asbestos tape to reduce the size of the thermal protection for the plasma torch.

The solid shaft of the specimen rotating mechanism was replaced with a hollow shaft to permit passage of thermocouple lead wires from the metal substrates of the specimens to a 12-channel slip ring assembly. An existing 12-channel slip ring assembly was adapted to the rotating mechanism as shown in the left background of Figure 12 and is driven by the rotating mechanism shaft through a hollow quill shaft. Thermocouple data are recorded on a multipoint strip chart recorder at the rate of approximately one point per second.

4.2.4.2 Specimen Fabrication

One set of eight abradability specimens was sprayed on metal substrates heated to 728°K (850°F). Insulation was installed on the outside diameter of two of the eight specimens to shield them from the propane burners and provide specimens sprayed on a lower temperature substrate for comparison purposes. The measured substrate temperature of these two parts was 589°K (600°F).

The same spray parameters, i.e., voltage, amperage, gas flows, powder feed rates, standoff distance, specimen surface speed and plasma gun traverse rate used for the NAS3-19759 specimens were also used for these specimens. The burner operating conditions were maintained constant to provide a constant temperature environment on the back of the specimens during spraying. The temperature of the substrate of the uninsulated specimens initially at 728°K (850°F), cooled during spraying while the insulated specimens, initially at 589°K (600°F), heated during spraying as shown in Figure 13. This data indicates that the effective temperature of the spray process was between 589 and 728°K (600 and 850°F). The effective temperature during the spraying of each of the layers appears to be different.

The gradual reduction in the initial substrate temperature for subsequent layers shown in Figure 13, points A through C and D through F, is attributed to gradual degradation of the performance of several of the propane burners caused by the undetected change in position of the fuel-air ratio control rings due to vibration.

4.2.4.3 Microstructural Evaluation

One specimen each of the specimens sprayed on substrates heated to 589°K (600°F) and 728°K (850°F) was microsectioned and compared with the microstructure of the final seal configuration evaluated under NAS3-19759. Typical microsections of each layer of each specimen are shown in Figures 14 through 16. Generally, the microstructures indicate that the effects of spraying on heated substrates are to increase the metallic fraction in the ZrO_2/CoCrAlY layers and reduce the porosity of the ZrO_2 layer.

The microstructural examinations also indicated excellent uniformity in layer thicknesses. Layer thicknesses were uniform within less than 0.06 mm (0.002 in).

4.2.4.4 Residual Stress Determination

Residual strain measurements were made on one of the abradability specimens sprayed on a substrate heated to 728°K (850°F) using the incremental removal method used under NAS3-19759. Strain changes were measured on the metal substrate surface at the center of the specimen between the mounting rails. A strain gage rosette with the perpendicular legs parallel with the circumferential and axial directions was used. The sprayed system was removed in predetermined increments by grinding with a diamond grit wheel. The specimen was clamped against a fixture which was machined to match the as-sprayed curvature of the specimen mounting rails during grinding to ensure removal of uniform thickness increments. The specimen was unclamped after removal of each increment to read the strains. The strain change associated with the removal of each increment was determined by subtracting the strain reading before removal of the increment from the reading after increment removal.

Prior to initiating machining, the specimen was clamped and unclamped several times to obtain an indication of the repeatability of the strain readings. Readings generally repeated within 15×10^{-6} cm/cm.

Since this experiment spanned a relatively long time, ambient temperature was recorded during grinding of the specimen and accounted for in the residual stress analysis. The specimen was assumed isothermal at the average ambient temperature during removal of each particular element for analytical purposes. Variations in ambient temperature during this experiment were found to affect the calculated residual stresses by less than two percent and were therefore not accounted for in subsequent tests.

Measured average ambient temperatures, increment thicknesses and strain change due to removal of the increment are shown in Table III. The axial strain gage failed after the seventh increment.

Residual stress distribution in the specimen was calculated using an infinite flat plate composite material model to determine a stress free temperature distribution through the specimen which would match the measured strains at the gage location in the circumferential direction. The stress free temperature distribution is the temperature distribution necessary to produce a zero stress distribution throughout the part. This stress free temperature distribution was then used in a model simulating the axial direction geometry. Calculated stresses in both directions were then combined analytically to account for the differences in the model assumptions, i.e., equal strain in mutually perpendicular directions, and the actual case to estimate the stresses in the actual specimen using the following relationships:

$$\sigma_{circ} = \frac{\sigma_{circ_{F.P.}} + \nu (1 - \nu)\, \sigma_{axial_{F.P.}}}{1 - \nu^2}$$

$$\sigma_{axial} = \frac{\sigma_{axial_{F.P.}} + \nu (1 - \nu)\, \sigma_{circ_{F.P.}}}{1 - \nu^2}$$

where:

σ_{circ}	=	stress in circumferential direction in specimen, N/m^2 (psi)
σ_{axial}	=	stress in axial direction in specimen, N/m^2 (psi)
$\sigma_{circ_{F.P.}}$	=	stress calculated in flat plate with circumferential direction stiffness, N/m^2 (psi)
$\sigma_{axial_{F.P.}}$	=	stress calculated in flat plate with axial direction stiffness, N/m^2 (psi)
ν	=	Poisson's ratio

Radial stresses were neglected since they were small.

The specimen stiffness in the circumferential direction in the area of the mounting rails, where the cross-section is non-uniform, was simulated in the flat plate model by assuming a material layer of the same thickness as the radial dimension of the sections of the mounting rails, i.e., rails and feet, and scaling the substrate modulus of elasticity by the ratio of the width of the rails or feet respectively divided by the width of the main body (platform) of the specimen. Other properties, i.e., coefficient of thermal expansion, thermal conductivity, density and Poisson's ratio, were assumed identical to the metal substrate properties.

The effect of mounting rails and specimen curvature on stiffness in the axial direction were neglected.

Calculated residual stresses at the ZrO_2 layer surface significantly exceeded the tensile strength of the ZrO_2 material measured under NAS3-19759. Since the physical parts were not cracked or otherwise failed, the analytical modeling and residual strain measurement experiment were examined more closely. It was known that the total strain at the gage location was equal to the sum of elongation and bending components which were oppositely directed. For the particular specimen configuration used in this experiment, these strain components were almost the same magnitude at the strain gage location in the circumferential direction. This meant that the calculated stresses would be very sensitive to small errors in the measured strains. Also, since the measured strain change in several of the increments were equal to or less than the accuracy of the strain instrumentation system, it is considered highly probable that this sensitivity was responsible for the unrealistic calculated residual stresses.

Further evaluation indicated that the differential between the elongation and bending strain components could be increased by approximately a factor of 15 by removal of the mounting rails or using a flat plate as was done in the NAS3-19759 experiments. This would greatly reduce the sensitivity of the calculated stresses to small errors in the strain measurements.

Earlier analytical results presented in Figure 11 indicate that the higher the substrate temperature the better the probability of developing desired levels of compressive residual stress to offset tensile cyclic thermal operating stresses. A substrate temperature of 922°K (1200°F) was selected for fabrication of specimens for a more complete evaluation of the benefits of residual stress management on seal system performance. It was also decided to spray future residual stress specimens on substrates with the support rail removed to increase the measureable strain at the gage location and more accurately define the corresponding residual stress.

4.3 COMPLETE SEAL SYSTEM EVALUATION

4.3.1 Specimen Configuration

Two sets of rig test specimens were fabricated, one with a 922°K (1200°F) substrate temperature and one without supplemental heating of the substrate. The sprayed seal configuration was identical to the final NAS3-19759 seal configuration in accordance with the conclusion of the optimization study discussed earlier. The metal substrate platform thickness was increased from 0.127 cm (0.050 in) to 0.254 cm (0.100 in) nominal to achieve a substrate stiffness greater than a 0.381 cm (0.150 in) thick flat plate to provide the desired level of compressive residual stress (Refer to Figure 10). The abradability specimen substrate with a 0.254 cm (0.100 in) thick platform has a circumferential stiffness equivalent to a 0.572 cm (0.225 in) thick plate.

The substrate temperature was maintained at 922°K (1200°F) as closely as possible during spraying of the heated parts. Burner gas flow had to be increased during spraying of each layer to maintain the temperature measured on the metal substrate surface constant. This tends to substantiate the earlier observation that the effective temperature of the plasma spray process is less than 922°K (1200°F).

The specimens fabricated without supplemental heating of the substrate (baseline system) were subjected to three preheat passes of the plasma torch without powder flow prior to spraying each layer of seal system material. This raised the temperature on the metal substrate surface (outside diameter) to approximately 333-339°K (140-150°F) at the initiation of deposition of each layer. The substrate surface temperature increased during spraying of each layer until it approached an equilibrium temperature of approximately 450°K (350°F).

Specimens for abradability, erosion and thermal shock rig tests were machined to remove coating pyramiding at the edges and to reduce abradability and thermal shock test specimens to design ZrO_2 layer thickness. All of the baseline system abradability and thermal shock test specimens cracked in the ZrO_2/CoCrAlY layers at both ends immediately after completion of machining. One of the 922°K (1200°F) seal system abradability test specimens also developed a laminar crack in the ZrO_2/CoCrAlY layers at one corner during machining. These specimens were ground without coolant to minimize contamination of the porous ceramic coating. It was suspected that the cause of these failures was the machining procedures used since similar parts have been machined with coolant under related P&WA programs without apparent distress.

A spare baseline system specimen was machined using coolant to investigate this possibility. This part showed no evidence of laminar cracking after machining. Although not conclusive proof that grinding without coolant may have generated excessive thermal stresses, it does tend to substantiate this conclusion.

4.3.2 Residual Stresses

Two specimens modified for residual stress measurement experiments were included in each set of parts. The mounting rails on the residual stress specimens were removed except four pairs of 0.254 cm (0.100 in) long equally spaced sections necessary for securing the specimens during removal of the sprayed system. This modification reduced the equivalent circumferential stiffness to that of a flat plate with the same thickness as the substrate platform to amplify the strains at the substrate surface to a more measurable level, as previously discussed.

It was recognized that the residual stress of the specimen with mounting rails removed would be different from the residual stress of the specimen with rails intact because of the differences in stiffness of the metal substrate. Residual stresses were assumed to be totally dependent on the thermal history of the parts during spraying. For this reason the stress free temperature distribution was assumed to be the same for both specimen configurations.

The change in the radius of curvature of the metal substrates due to deposition of the sprayed system was measured on the residual stress specimens to provide a preliminary indication of the average stress state in the sprayed system. The radius of curvature of both sets of specimens increased due to deposition of the plasma sprayed coating system as shown in Table IV. The change in curvature of the 922°K (1200°F) parts was approximately three times the curvature change for the baseline parts. This indicates that the average stress in the sprayed system for both sets of parts is compressive, with a significantly higher stress in the 922°K (1200°F) parts.

Residual stresses calculated in the 40/60 ZrO_2/CoCrAlY layer of the baseline system specimen exceeded the strength of the 40/60 ZrO_2/CoCrAlY material by approximately 30 percent. Since cracks were not observed in this layer in the as-sprayed state the residual strain data was reviewed. Layer thicknesses measured from the machined edges of abradability and thermal shock rig test specimens which were sprayed at the same time were compared with thicknesses determined during machining of the residual stress specimen. It appears that layer interfaces were missed during machining of the residual stress specimen. Several of the increments included two layer materials. Resolution of the effect of each material in these increments was unsuccessful. Therefore, this data is considered invalid. Repetition of the residual stress measurement experiment for this configuration is required to estimate actual stresses in this system and to quantify the benefits of prestress management.

Residual strains measured on a 922°K (1200°F) system specimen are shown in Table V. Analysis of this data indicates circumferential and axial strains are essentially maximum and minimum principal values. Circumferential strain data was reduced to obtain stress free temperature distribution through the residual stress specimen. The substrate was assumed stress free at 922°K (1200°F). The stress free temperature in each increment was iteratively determined to match the negative of the measured strain change at the gage location as the seal was analytically rebuilt. The calculated stress free temperature distribution radially through the residual stress specimen is shown in Figure 17. This distribution was estimated using material properties data obtained under NAS3-19759. Properties data for materials sprayed on 922°K (1200°F) metal substrates was obtained as discussed later. Figure 18 shows the stress free temperature distribution obtained from the same strain data using the new properties. A comparison of Figures 17 and 18 provides an evaluation of effects of property variability on stress free temperatures.

4.3.3 Material Properties

Modulii of elasticity and rupture, strain to failure, thermal expansivity and thermal conductivity were determined for each of the plasma sprayed ceramic and ceramic-metal layers in the seal system. Samples were machined from specimens sprayed on metal substrates heated and maintained at 922°K (1200°F). All specimens except thermal conductivity specimens were sprayed on mild steel substrates which were removed with dilute (50% solution) nitric acid during machining of test samples. Thermal conductivity specimens were sprayed on Hastelloy X substrates.

4.3.3.1 Modulii of Elasticity and Rupture and Strain to Failure

Modulii of elasticity and rupture and strain to failure were determined at room temperature and at the maximum estimated operating temperature for each of the sprayed ZrO_2/CoCrAlY layers and the ZrO_2 layer using the four-point flexure method. A strain gage, placed at midspan and center of each specimen, was used to measure specimen deflection for room temperature tests. Measurement of cross-head deflection was used to determine specimen deflection at elevated temperatures. Test specimens measured 0.254 X 0.762 X 3.556 cm (0.1 X 0.3 X 1.4 in) and were prepared such that the length of the specimen was in the circumferential direction. Elevated temperature characteristics were determined at 1589°K (2400°F) for the ZrO_2 layer and 1256°K (1800°F) for the 85/15 and 40/60 ZrO_2/CoCrAlY layers.

Modulus of elasticity was calculated using either of the following formulii as applicable:

For strain gaged specimens:

$$E = \frac{35\,(P/\epsilon)}{4\,b\,h^2}$$

where: E = elastic modulus

P/ϵ = slope of the load versus strain curve

b = specimen width perpendicular to the load application

h = specimen thickness coincident with the load direction

For elevated temperature tests where the cross head deflection was measured:

$$E = \frac{S^3\,(P/\epsilon)}{8\,b\,h^3}$$

where: S = distance between supports

P/ϵ = slope of the load versus deflection curve

Modulus of rupture was calculated using:

$$\sigma_u = \frac{3\,P\,S}{4\,b\,h^2}$$

where: σ_u = modulus of rupture (bending strength)

P = maximum load prior to specimen failure

Strain to failure was read directly for strain gaged specimens. For deflectometer measured specimens, strain to failure (ϵ_u) was calculated using:

$$\epsilon_u = \frac{6h\,X}{(S-a)\,(S + 2a)}$$

where: a = ½ distance between supports (S/2)

X = deflection at load points at failure (deflectometer reading)

Test data for the materials sprayed on metal substrates heated and maintained at 922°K (1200°F) are summarized in Table VI. These results indicate:

1. The rupture modulii for the ZrO_2 and 85/15 ZrO_2/CoCrAlY materials tend to increase with increasing temperature.

2. The moduli of elasticity and strain to failure for the ZrO_2, 85/15 ZrO_2/CoCrAlY and 40/60 ZrO_2/CoCrAlY materials and the modulus of rupture for the 40/60 ZrO_2/CoCrAlY material tend to decrease with increasing temperature.

3. Both elastic and rupture moduli tend to increase with increasing metallic fraction.

Data measured on materials sprayed without supplemental heating of the metal substrate under contract NAS3-19759 reported in NASA CR-135183 (PWA-5521) is reproduced in Table VII for comparison purposes. Comparing the data in Table VI with comparable data in Table VII indicates spraying on a heated substrate tends to:

1. Reduce rupture moduli at room temperature and increase rupture moduli at elevated temperature except for the 40/60 ZrO_2/CoCrAlY which decreased at elevated temperature.

2. Increase elastic moduli at room temperature and elevated temperature except room temperature ZrO_2 modulus and elevated temperature 40/60 ZrO_2/CoCrAlY modulus which decreased.

3. Reduce room temperature and increase elevated temperature strains to failure with the higher metallic fraction materials exhibiting the largest change.

In general, the effect of spraying on a heated metal substrate on rupture and elastic moduli is significant and will significantly affect calculated stresses and stress-strength ratios in the seal system, as will be seen.

4.3.3.2 Thermal Expansivity

The thermal expansivity for each material layer in the plasma sprayed ZrO_2/CoCrAlY seal system sprayed on 922°K (1200°F) metal substrates was measured in the circumferential direction. Specimens measured 3.556 X 0.762 X 0.254 cm (1.4 X 0.3 X 0.1 in).

After being accurately measured in the 3.556 cm (1.4 in) direction, the specimens were instrumented with a Netzch Electronic Automatic Recording Dilatometer. The system was placed in the center zone of a closed chamber which was evacuated and then backfilled with helium. The specimens were then programmed for temperature rise and equilibrium at approximately 100°K (180°F) intervals from 293°K (68°F) to 1202°K (1704°F), 1341°K (1954°F) and 1608°K (2434°F) for 40/60 ZrO_2/CoCrAlY, 85/15 ZrO_2/CoCrAlY and ZrO_2 materials, respectively. An equivalent program for temperature fall and equilibrium was also implemented. The rate of temperature rise and fall was approximately 5°K/min (9°F/min).

Results are summarized in Figures 19 through 22 along with data measured under contract NAS3-19759 for materials sprayed without supplementary substrate heating for comparison. The 40/60 and 85/15 ZrO_2/CoCrAlY materials demonstrated fairly repeatable thermal growths both during heating and cooling and from cycle to cycle although some tendency to grow was seen.

The ZrO_2 material demonstrated a very definite shrinkage above 1373°K (2011°F) during the first thermal cycle, as shown in Figure 21. Total shrinkage of 0.36 percent was measured. Subsequent cycles did not exhibit this shrinkage and were very repeatable. Figure 22 shows data typical of these subsequent cycles.

With the exception of the ZrO_2 material, both sets of data correlate closely and indicate no appreciable effect of spraying on preheated substrates on the thermal growth characteristics of the ZrO_2/CoCrAlY materials.

The slope of the ZrO_2 thermal growth curve measured under this program is slightly steeper than the NAS3-19759 curve and the net shrinkage is larger. The NAS3-19759 data measurement was aborted twice when significant departure from linearity was noted. This probably accounts for most of the net shrinkage data difference since the NAS3-19759 data is from the third cycle, after part of the shrinkage had already occurred. The cause of the difference in slope is not apparent.

The mean coefficient of thermal expansion was calculated from the thermal expansivity data shown in Figures 19 through 22 relative to any selected stress free temperature using:

$$\alpha_{T_{sF}} = \frac{(\Delta L/L)_T - (\Delta L/L)_{T_{sF}}}{[1 + (\Delta L/L)_{T_{sF}}]\,(T - T_{sF})}$$

where:

$\alpha_{T_{sF}}$ = mean coefficient of thermal expansion from T_{sF} to T

$(\Delta L/L)_T$ = unit thermal expansion from T_o to T

$(\Delta L/L)_{T_{sF}}$ = unit thermal expansion from T_o to T_{sF}

T_o = initial temperature from which thermal expansion data was measured

T = temperature at which measurement was made

T_{sF} = stress free temperature

4.3.3.3 Thermal Conductivity

Thermal conductivity was measured on samples of the ZrO_2 layer and the complete seal system. Both samples were sprayed on 922°K (1200°F) Hastelloy-X substrates which had been plasma spray coated with 0.0762 - 0.127 mm (0.003 - 0.005 in) thick NiCrAl bond coat. Test samples were machined to 2.54 cm (1 in) diameter and both disk faces were machined flat and parallel within 0.0508 mm (0.002 in) full indicated runout relative to the coating-substrate interface and each other.

Both specimens were tested using the comparative cut bar method. A specimen was placed between two Inconel 702 reference standards of known thermal conductivity with thermocouples at the interfaces. The test stack was placed between the plates of an upper heater, auxiliary heater and a lower heat sink. A reproducible load was applied to the top of the complete system to achieve a uniform interface contact. A guard tube which could be heated or cooled was placed around the system and the interspace and surroundings were filled with an insulating powder. By adjusting the heaters and heat sink temperatures, a constant temperature distribution was maintained in the system. Radial heat losses were reduced to negligible values by keeping the guard tube temperature close to the average temperature of the sample. Temperatures at various locations in the system were recorded when the equilibrium conditions were attained at four average specimen temperatures between 373°K (212°F) and 1473°K (2192°F) during heatup and two average temperatures during cool down. The thermal conductivity of each specimen was calculated using:

$$K_S = \frac{1}{2} \frac{(X_S)}{(T_S)} \left[\frac{(K_{R_1} T_{R_1})}{(X_{R_1})} + \frac{(K_{R_2} T_{R_2})}{(X_{R_2})} \right]$$

where: K = thermal conductivity
X = thickness
T = temperature difference
S = specimen
R_1 = top reference
R_2 = bottom reference

Subsequent to testing, individual layer and substrate thicknesses were determined and thermal conductivities of the sprayed coatings were then calculated using the resistance method:

$$K_c = \frac{X_c}{\frac{X_s}{K_s} - \frac{X_m}{K_m}}$$

where: c = coating
m = substrate

Thermal conductivities of the mixed ZrO_2/CoCrAlY intermediate layers were estimated from these results by:

1. Calculating the average thermal conductivity of the composite of the two intermediate layers using:

$$K_I = \frac{X_I}{\dfrac{X_T}{K_T} - \dfrac{X_c}{K_c}}$$

where:

K_I	=	composite average thermal conductivity of intermediate layers
K_T	=	average thermal conductivity of total coating system
K_c	=	thermal conductivity of sprayed ZrO_2 layer
X_I	=	intermediate layers thickness
X_T	=	total coating thickness
X_c	=	ZrO_2 layer thickness

2. Plotting the thermal conductivity against intermediate layer thickness assuming:

   - the thermal conductivity at the ZrO_2 layer-intermediate layer interface is equal to the ZrO_2 layer conductivity,
   - the thermal conductivity at the intermediate layer-metal substrate interface is equal to the substrate conductivity, and
   - the thermal conductivity at the mean thickness of the intermediate layers equals K_I calculated in step 1.

3. The thermal conductivity of each of the intermediate layers was taken as the value of the curve drawn through the foregoing points at the center of each layer.

Estimated thermal conductivities for each of the 922°K (1200°F) ZrO_2/CoCrAlY seal system layers are shown in Figure 23. Thermal conductivity data for the NAS3-19759 seal system which was sprayed on unheated metal substrates is also shown in Figure 23 for comparison. This data indicates that spraying on heated metal substrates tends to increase the thermal conductivity of all layers. The ZrO_2/CoCrAlY layers tend to increase more than the ZrO_2 layer. This tends to agree with metallography results which indicate increased ZrO_2 layer density and increased metallic fraction in the ZrO_2/CoCrAlY layers which would be expected to increase the thermal conductivity in all layers.

4.3.3.4 Hardness

Superficial Rockwell 45Y hardness was measured on the as-sprayed ZrO_2 surface of all abradability and erosion specimens, both those sprayed with and without supplemental heating of the metal substrates. Measurements were taken at fifteen locations on the abradability specimens and at nine locations on the erosion specimens. After grinding the coating surface and edges for rig testing as previously discussed, hardness measurements were repeated on three abradability specimens that had been sprayed onto 922°K (1200°F) substrates.

The difference in processing, i.e., spraying with or without supplemental preheating, did not significantly affect the as-sprayed hardness of the abradability specimens. The average hardness of eight specimens from each set was 74.4 for specimens sprayed without supplemental substrate heating and 75.7 for specimens sprayed on 922°K (1200°F) substrates. Scatter in the individual specimens average hardness for specimens sprayed without supplemental substrate heating was approximately one-half the scatter for specimens sprayed on 922°K (1200°F) substrates, ±1.05 vs. ±2.1.

Erosion specimens did not agree as closely. The average hardness of two specimens from each set was 73.5 for specimens sprayed without supplemental substrate heating and 69.0 for specimens sprayed on 922°K (1200°F) substrates. The cause for the larger difference is not known.

The average hardness of three abradability specimens sprayed on 922°K (1200°F) substrates increased from 74.3 as-sprayed to 88.3 after machining. This increase in hardness is attributed primarily to the reduction in roughness of the ZrO_2 surface.

4.3.4 Abradability Test Results

The capability of the sprayed seal system to tolerate blade tip rubs without catastrophic failure was evaluated by abradability rig tests. Tests were conducted under simulated engine conditions of seal surface temperature, blade tip speed and incursion rate.

All abradability tests were performed with P&WA's high temperature abradability test rig shown in Figure 24. Twelve simulated turbine blade tips were mounted in the periphery of a disk driven at the required speed by a compressed air turbine. The seal segment specimen was mounted in a fixture at the end of a horizontal post attached to a movable carriage assembly. The carriage assembly injects the specimen radially into the rotor assembly at the required incursion rate. The seal specimen was heated from both sides of the rotor by oxygen-acetylene torches directed at the seal surface. Heating torches were also mounted off the carriage assembly. Gas flows and distance between the torches and seal specimen was varied to control the seal surface temperature.

Seal surface temperature was monitored by optical pyrometers. Carriage travel was monitored by a linear differential transformer. A load cell in the carriage feed system permitted determination of the average normal force between the seal specimen and blade tips. All data were recorded continuously on a strip chart.

Blade tip and seal wear was determined through pre- and post-test measurements. Relative abradability between different specimens and different seal systems was assessed on the basis of the volume wear ratio (VWR); the blade tip wear volume divided by the seal wear volume. The smaller the volume wear ratio, the better the abradability of the seal system.

Abradability test results are generally the same as experienced under NAS3-19759 for similar test conditions and substantiate the effect of incursion rate on blade wear, i.e., the higher incursion rate resulted in increased blade wear. These results also indicate that spraying the seal coating system on a 922°K (1200°F) substrate did not significantly affect the abradability of the ZrO_2 layer.

Four abradability tests were attempted as summarized in Table VII. The first two specimens, one a machined 922°K (1200°F) seal system specimen and the other an as-sprayed baseline seal system specimen developed laminar cracks and spalled severely during heatup to test conditions.

Spallation that resulted during heatup of the first two specimens is attributed to excessive heating of the metal substrates. In an attempt to rub the specimens off-center to permit two tests on a single specimen, flame impingement from one torch was on the side instead of the ZrO_2 surface of the specimen and overheated the metal substrate.

The third and fourth specimens were as-sprayed 922°K (1200°F) seal system specimens. The third specimen was rubbed at 1589°K (2400°F) surface temperature and 284.4 m/s (933 ft/sec) with twelve B-1900 cast nickel alloy blades at an incursion rate of 0.0254 mm/s (0.001 in/sec). The blades wore a groove 0.508 mm (0.020 in) deep in the seal with an average blade tip wear of 0.061 mm (0.0024 in), yielding a volume wear ratio of 0.166. The ZrO_2 layer of this specimen spalled along one side outside the rub path during heatup to test conditions. During the rub interaction additional sections of the ZrO_2 layer at both ends of the specimen also spalled. However, approximately 75 percent of the rubbed area remained intact as shown in Figure 25. A thin layer of blade tip material transfer was evident in the seal wear groove.

The fourth specimen was tested at 1589°K (2400°F) seal surface temperature, 304.8 m/s (1000 ft/sec) blade tip velocity and 0.254 mm/s (0.010 in/sec) incursion rate. Heavy blade tip wear and transfer to the seal specimen occurred as shown in Figure 26. The incursion rate gradually slowed down to 0.109 mm/s (0.0043 in/sec) as the rub interaction proceeded indicating the maximum reaction load was insufficient to maintain the wear rate.

4.3.5 Erosion Test Results

Erosion resistance of one specimen of each of the plasma sprayed ZrO_2/CoCrAlY seal systems, i.e., sprayed with and without metal substrate heating, was evaluated by hot particulate rig testing at a ZrO_2 surface temperature of 1589°K (2400°F) and an impingement angle of 0.262 rad (15°).

Erosion tests were performed in the hot particulate erosion rig shown in Figure 27. The specimen was positioned at a distance of 3.81 cm (1.5 in) and specified impingement angle relative to the end of the combustor exit nozzle by a compound vise. The specimen was heated by impinging JP-5 fuel and air combustion products on the ZrO_2 surface of the specimen through a 1.905 cm (0.75 in) diameter exit nozzle. Specimen temperature and exit gas velocity were controlled by varying fuel and air flows.

After the specimen temperature and gas velocity were stabilized, particulate flow was initiated. The 80 grit Al_2O_3 particulate was gravity fed into a tube connected into the combustor exit nozzle approximately 5.08 cm (2 in) upstream of the nozzle end where it was picked up and accelerated to the specimen surface by the hot gas stream. Particulate flow rate was controlled by a precalibrated orifice in the storage hopper discharge line. The weight of particulate used and the duration of particulate flow during the test was monitored to check the particulate flow rate.

Specimen temperature was measured optically on the ZrO_2 surface. Erosion wear was determined by measuring the weight loss of the specimen at five minute intervals.

The erosion specimen consisted of the composite seal system sprayed on a flat Hastelloy-X plate nominally 3.81 by 5.08 by 0.254 cm (1.5 by 2.0 by 0.1 in). A 3.81 cm^2 (1.5 in^2) section of the substrate is sprayed, leaving a 1.27 cm (0.5 in) uncoated end for mounting in the test fixture.

Test results are summarized in Table IX and Figure 28.

The particulate flow rate used for these tests was 20 percent of the rate used for the NAS3-19759 tests. In view of this, a comparison with previous data could not be made.

The ZrO_2 layer of the baseline seal system cracked severely during heatup for the second five minute test interval due to an accidental rapid thermal shock and it delaminated during cooldown after completion of the test interval. Therefore, the erosion rate could not be estimated. The measured data point at five minutes is shown in Figure 28.

4.3.6 Thermal Shock Test Results

The durability of the sprayed ZrO_2/CoCrAlY seal system in an engine application will depend greatly on its capability to successfully survive the initial and subsequent thermal cycles corresponding to the engine operational conditions. This is the most difficult parameter to satisfy with a ceramic seal because of the relatively low strength (especially tensile strength) of ceramic materials and the large mismatch in thermal growth between ceramic and metallic materials. The graded, layered system was designed specifically to modify the layer difference in thermal expansion between the metal substrate and ceramic. Thermal and mechanical properties of each of the individual layers in the graded ZrO_2/CoCrAlY structure and the metal substrate, as well as the geometry of the seal segment and residual stress state, affects stresses generated during thermal cycling.

Thermal fatigue characteristics were evaluated by rig tests which subjected the seal specimens to a simulated gas turbine engine cycle from idle to sea level takeoff (SLTO) and back to idle, shown in Figure 29. Appropriate temperature - time cycles were imposed on the ZrO_2 and metal substrate surfaces. A typical actual cycle is also shown in Figure 29 for comparison with the goal and illustrating the very close simulation produced by this rig. Heating and cooling rates to idle conditions were controlled to minimize associated thermal stresses. ZrO_2 and substrate surface temperatures were heated and cooled approximately linearly between room temperature and idle conditions over a five minute duration.

Earlier thermal shock tests results under contract NAS3-19759 indicated thermal stress cracking initiated very early during the test. Analysis indicated cracking could occur in the first thermal cycle during acceleration to SLTO. Therefore, prior to initiating the idle - SLTO test cycle, it was attempted to better define when and where cracking was initiating by subjecting the seal specimen to isolated portions of the cycle. The specimen was subjected to an initial heatup to idle and cooldown cycle and the initial acceleration heatup cycle shown in Figure 30 and thoroughly inspected after each cycle. The specimen was also inspected after the first complete thermal fatigue test cycle (Figure 29) and after 100, 300 and 500 cycles.

The thermal fatigue test rig is shown in Figure 31. The specimen was mounted in a water cooled copper fixture. A combination of oxygen-propane torches and cooling air jets were used to achieve the desired thermal cycles on the ZrO_2 and metal substrate surfaces. The torches were mechanically moved toward or away from the specimen at controlled rates to provide the required thermal cycle. Fixed cooling air jets were turned on or off or the flow was changed at predetermined intervals to meet the cycle requirements. The ZrO_2 and metal substrate surface temperatures were monitored continuously with an optical pyrometer and thermocouples, respectively, and recorded on a strip chart.

Four abradability specimens, three sprayed on metal substrates heated to 922°K (1200°F) and one sprayed without supplemental heating of the metal substrate, were thermal fatigue tested. Two of the three 922°K (1200°F) specimens were machined on the edges and ZrO_2 surface as previously discussed. The third 922°K (1200°F) specimen was an as-sprayed residual stress specimen with metal substrate rails modified to reduce the circumferential stiffness as described earlier. The specimen sprayed without supplemental heating was tested in the as-sprayed condition. Test results are summarized in Table X.

All of the 922°K (1200°F) seal specimens failed during the initial acceleration cycle. The two machined specimens with standard metal substrate configurations exhibited cracking after initial heatup to idle. The as-sprayed residual stress specimen showed no apparent distress after initial heating to idle but delaminated completely at the ZrO_2 - 85/15 ZrO_2/CoCrAlY interface after the initial acceleration cycle. This difference in behavior is attributed primarily to the substrate stiffness difference although factors such as ZrO_2 layer thickness difference and defects or stresses caused by machining could have also contributed.

The seal system sprayed without substrate heating completed 100 simulated engine cycles before crack initiation was observed. Further inspection after subsequent testing indicated laminar cracking did not initiate until after 100 cycles and before 300. Five hundred cycles were successfully completed without spallation and the specimen appearance was better than the post-test condition of previous configurations after only 100 cycles, as shown in Figure 32.

Radial cracks, Figure 33, were almost invisible without magnification. As shown by post-test metallography, Figure 34, radial cracks only propagated through approximately 60 percent of the ZrO_2 layer thickness. Laminar cracking at the ZrO_2 layer interface propagated from both ends approximately 1.9 cm (0.75 in). As shown in Figure 34, the laminar cracks tended to propagate along the ZrO_2 layer interface for approximately 0.6 cm (0.25 in) and then turned toward the ZrO_2 surface at a shallow angle.

4.3.7 Stress Analyses

Stress free temperature distributions calculated based on measured residual strains in ZrO_2/CoCrAlY seal system specimens sprayed on modified abradability specimen metal substrates with and without substrate heating were used to estimate stresses in the thermal fatigue specimens before and after testing.

Both steady state and transient temperature distributions radially through the seal specimen were calculated using the two-dimensional finite element computer program used for NAS3-19759 thermal analyses. Temperature distributions were calculated based on estimated or measured temperatures on the ZrO_2 and metal substrate surfaces and physical properties of the seal system materials. Temperatures were assumed uniform in the axial-circumferential plane so only radial gradients were calculated.

Calculated thermal distributions at selected instants in time were used in a two dimensional finite element plane stress computer program to estimate stress distributions. The same computer program used for NAS3-19759 analyses, modified under a P&WA funded program to approximate residual stress distributions by assignment of stress free temperatures to each area of the specimen, was used to calculate total stress distributions in the circumferential-radial and the axial-radial planes.

Stress distributions at critical cycle points; i.e., idle, six seconds into acceleration, SLTO and twelve seconds into deceleration; were calcualted for the estimated engine cycles using various combinations of materials properties and residual stress data. Subsequent to thermal fatigue testing, stress distributions at actual test conditions for the maximum thermal gradient point during initial idle and initial acceleration cycles were also calculated. Results of these analyses are summarized in Table XI. Circumferential stresses are reported since maximum stresses occurred in this plane.

Initial data, calculated using baseline material properties measured under NAS3-19759 with and without 900°K (1200°F) residual stresses, indicated stresses in the ZrO_2 layer would exceed its strength (indicated by stress-strength ratios greater than 1.0). Stresses in the intermediate layers were within their respective material strengths except the 40/60 ZrO_2/CoCrAlY layer at SLTO without residual stress. Subsequent calculations using measured properties for materials sprayed on 922°K (1200°F) substrates indicated reduced tensile and larger compressive stresses in the ZrO_2 layer and larger tensile and compressive stress-strength ratios in the 85/15 ZrO_2/CoCrAlY layer. Stresses calculated in both the ZrO_2 and 85/15 ZrO_2/CoCrAlY layers exceeded their respective material strengths when properties and measured residual stresses for the 922°K (1200°F) seal system are taken into account. Both tensile and estimated compressive strengths were exceeded. Compressive strengths for these analyses was estimated by multiplying the measured tensile strengths of the ZrO_2, 85/15 ZrO_2/CoCrAlY and 40/60 ZrO_2/CoCrAlY layers by factors of 4.0, 3.55 and 2.2 respectively. These factors were selected based on compressive strength data measured on sintered ZrO_2 metal materials under a related P&WA program which indicated the ZrO_2-metal materials compressive strength to tensile strength ratio was approximately a linear function of the ZrO_2 fraction between 1.0 for all metal to 4 or 5 for all ZrO_2.

A comparison of the results of analytical study 1) with 2) in Table XI will indicate the effect of the residual stress resulting from spraying on parts maintained at 922°K (1200°F). A comparison of case 2) with 3) illustrates the effect of physical property variation caused by spraying on a 922°K (1200°F) substrate.

Maximum (tensile) principal stresses in both the ZrO_2 and 85/15 ZrO_2/CoCrAlY layers for specimens sprayed onto 922°K (1200°F) substrates exceeded the tensile strength of the respective materials at the 13 second point in the actual initial acceleration cycle measured in the test rig. These stresses were calculated to occur at an angle of approximately 0.7854 rad (45°) relative to the layer interface. The crack path was at approximately 0.5236 rad (30°) relative to the interface as shown in Figure 35. The location of the calculated maximum and minimum principal stress-strength ratios for both idle and 13 second acceleration rig test cycle points are also shown in Figure 35.

Typical circumferential stress distributions are shown in Figure 36. Generally, incorporation of compressive residual stresses tended to reduce tensile stresses in the central area of the seal in all layers and have relatively small effect on tensile stresses near the edge as shown by comparison of curves A and B. Material properties changes caused by spraying the seal system on a 922°K (1200°F) substrate had a mixed effect on tensile stresses. ZrO_2 layer stresses tended to be reduced as shown by comparison of curves B and C. Intermediate layer stresses, especially in the 85/15 ZrO_2/CoCrAlY layer, were increased significantly as shown in Table XI. Magnitudes generally tended to increase as tensile stresses were reduced except in the intermediate layers where properties changes resulted in increasing magnitude of both tensile and compressive stresses.

It was not possible to complete the analyses for correlation with test results of the baseline seal system because of lack of accurate residual stress data. The residual stress measurement experiment on the baseline seal system should be repeated to correlate analysis with the successful test results on this system.

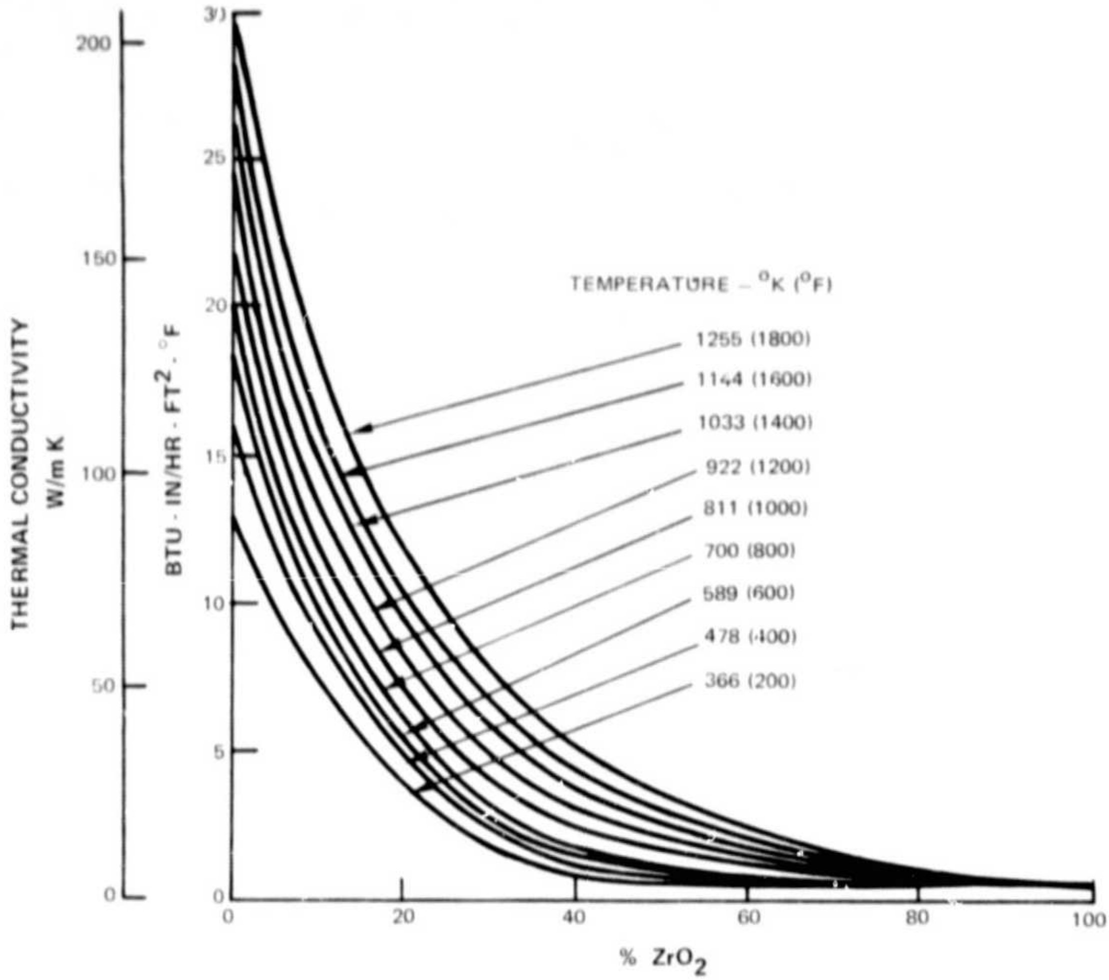

Figure 1 *Estimated Thermal Conductivity Variation Versus Spray Powder ZrO_2 Weight Fraction for Plasma Sprayed ZrO_2/CoCrAlY Materials*

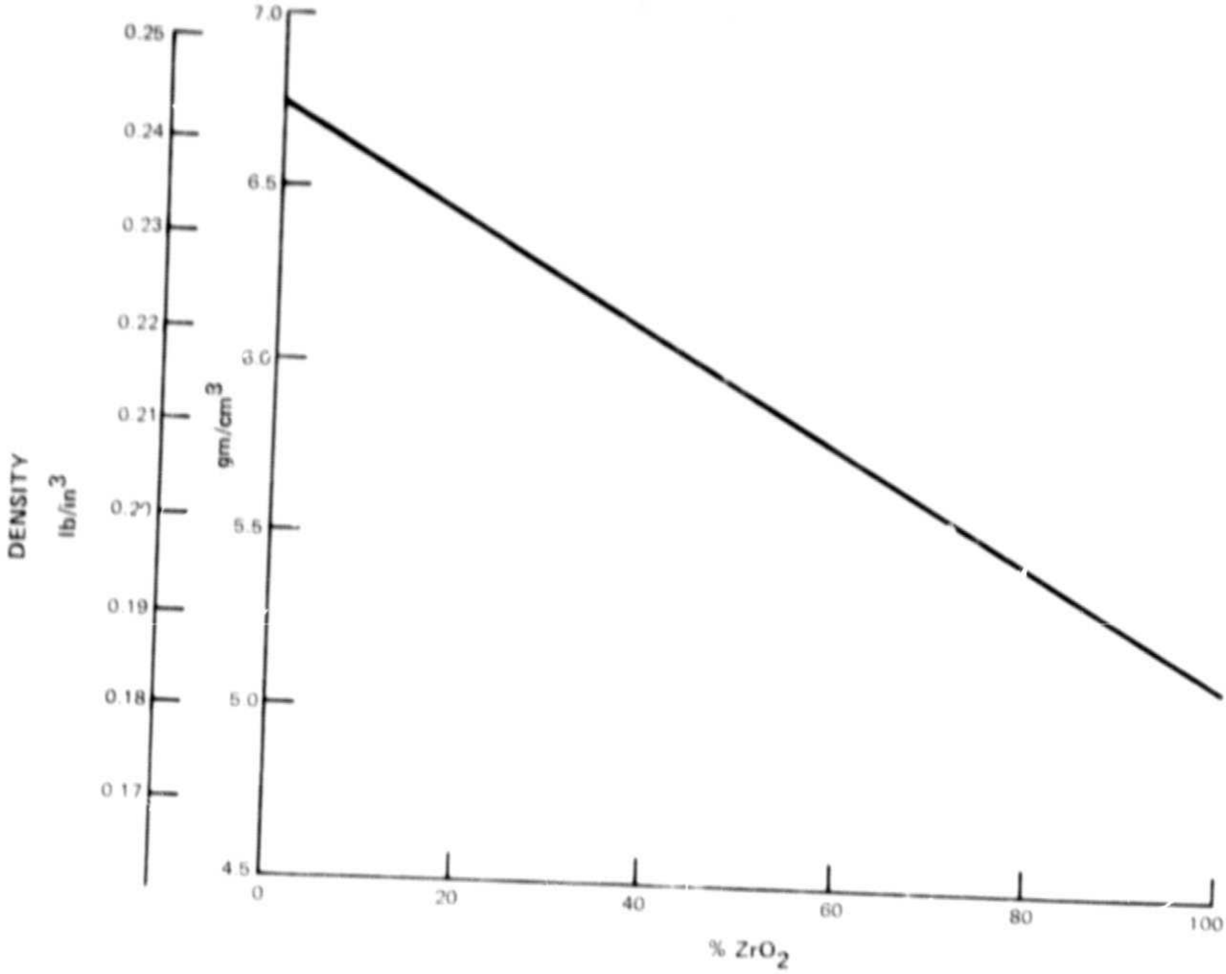

Figure 2 *Estimated Density Variation Versus Spray Powder ZrO_2 Weight Fraction for Plasma Sprayed ZrO_2/CoCrAlY Materials*

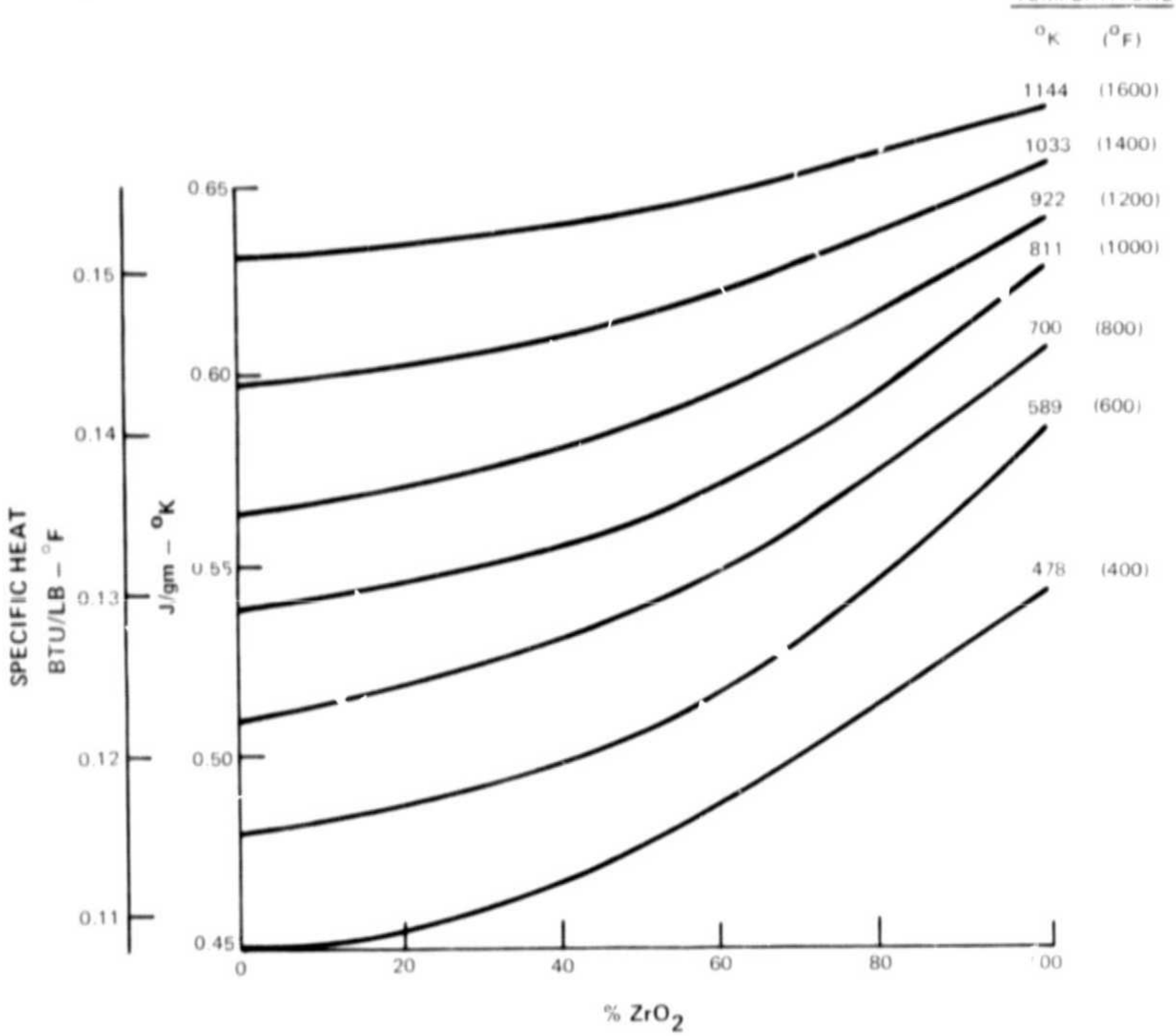

Figure 3 *Estimated Specific Heat Variation Versus Spray Powder ZrO_2 Weight Fraction for Plasma Sprayed ZrO_2/CoCrAlY Materials*

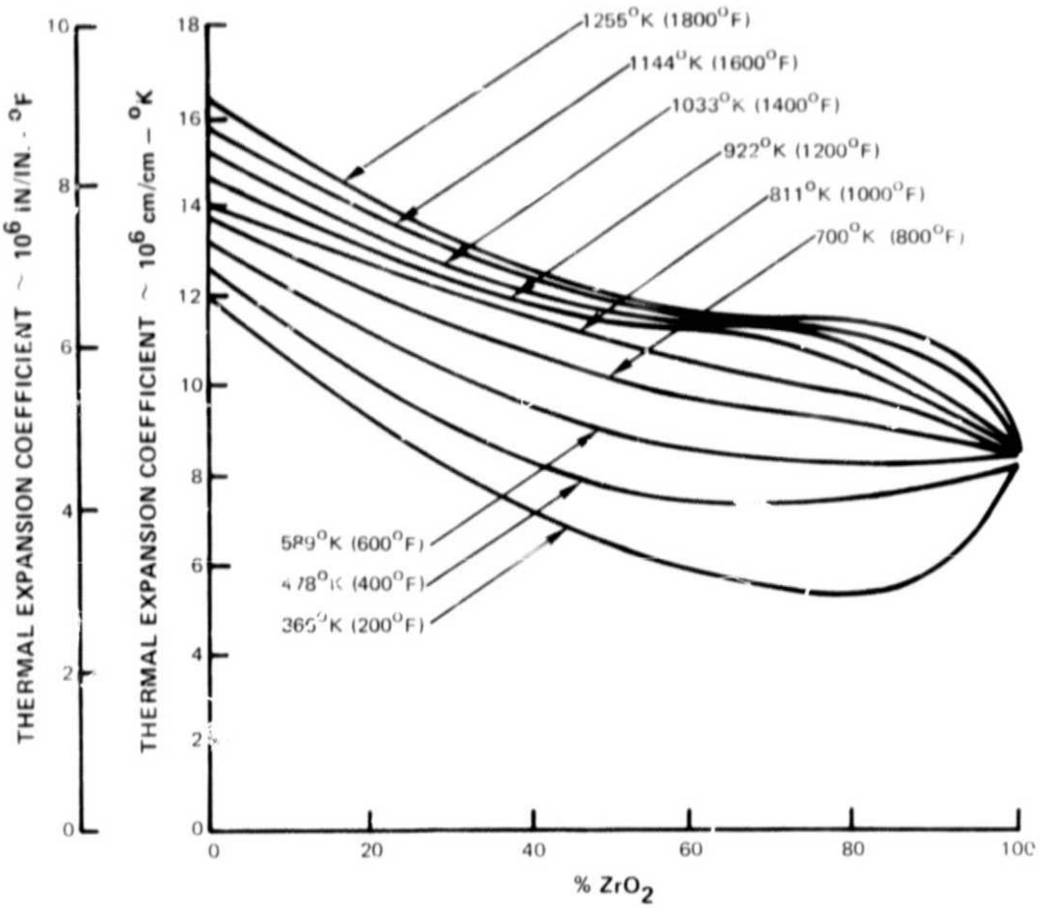

Figure 4 Estimated Thermal Expansion Coefficient Variation Versus Spray Powder ZrO_2 Weight Fraction for Plasma Sprayed ZrO_2/CoCrAlY Materials

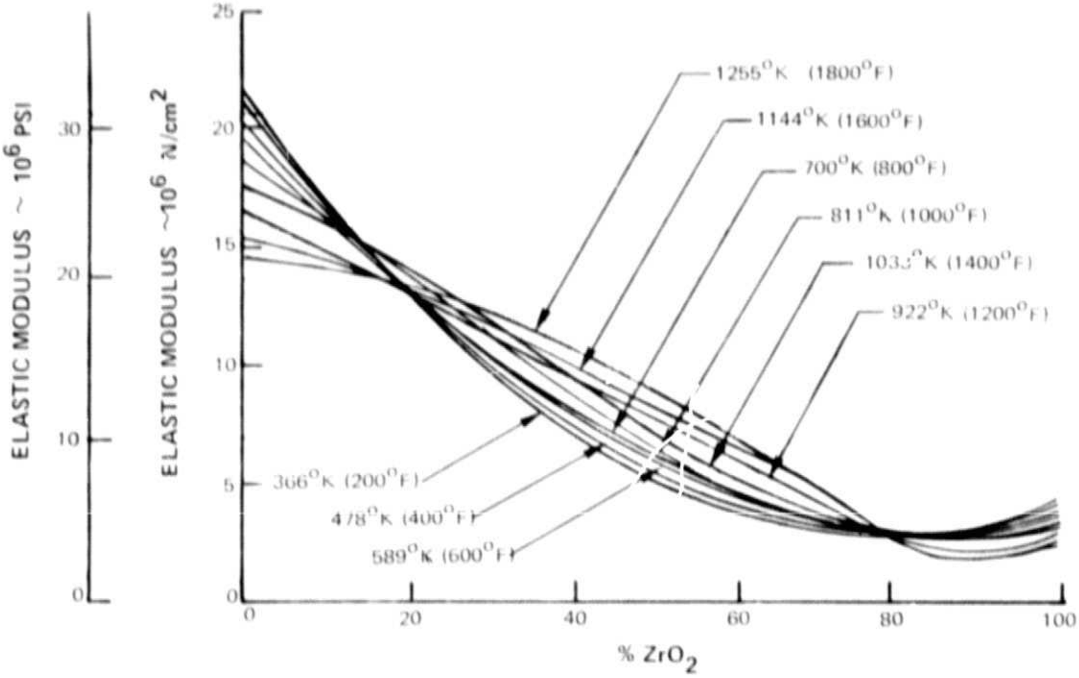

Figure 5 Estimated Elastic Modulus Variation Versus Spray Powder ZrO_2 Weight Fraction for Plasma Sprayed ZrO_2/CoCrAlY Materials

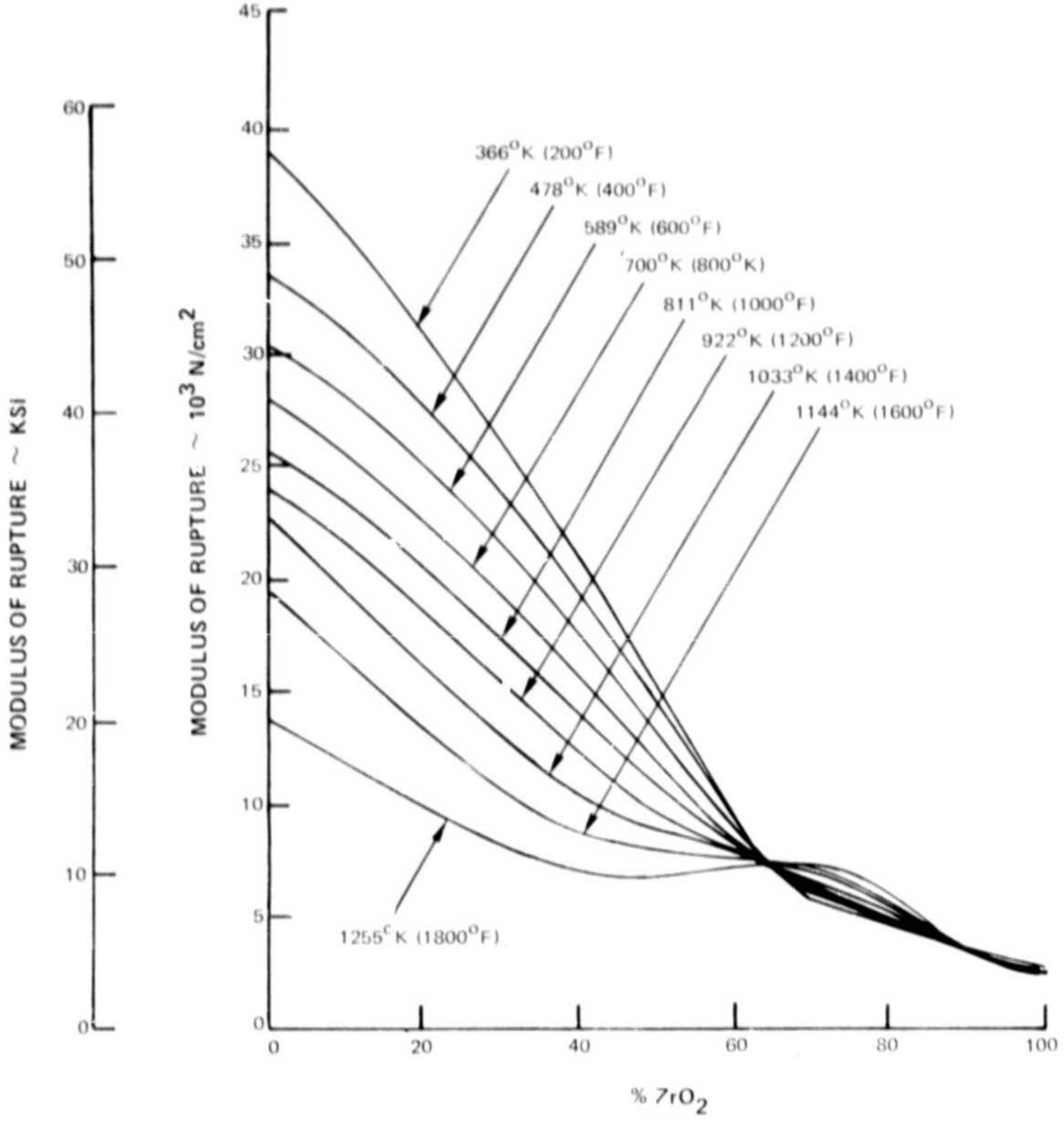

Figure 6 *Estimated Modulus of Rupture Variation Versus Spray Powder ZrO_2 Weight Fraction for Plasma Sprayed ZrO_2/CoCrAlY Materials*

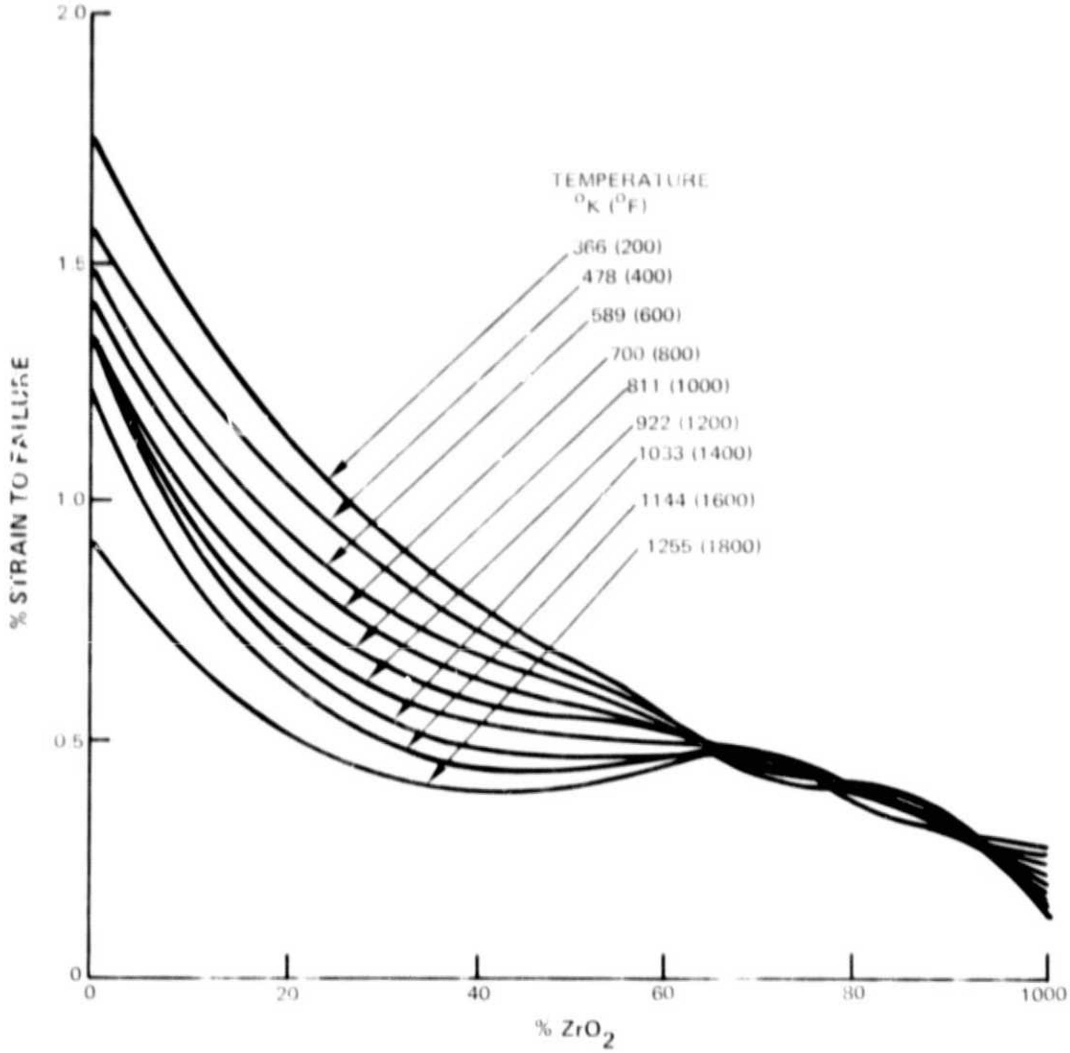

Figure 7 Estimated Strain To Failure Variation Versus Spray Powder ZrO_2 Weight Fraction for Plasma Sprayed ZrO_2/CoCrAlY Materials

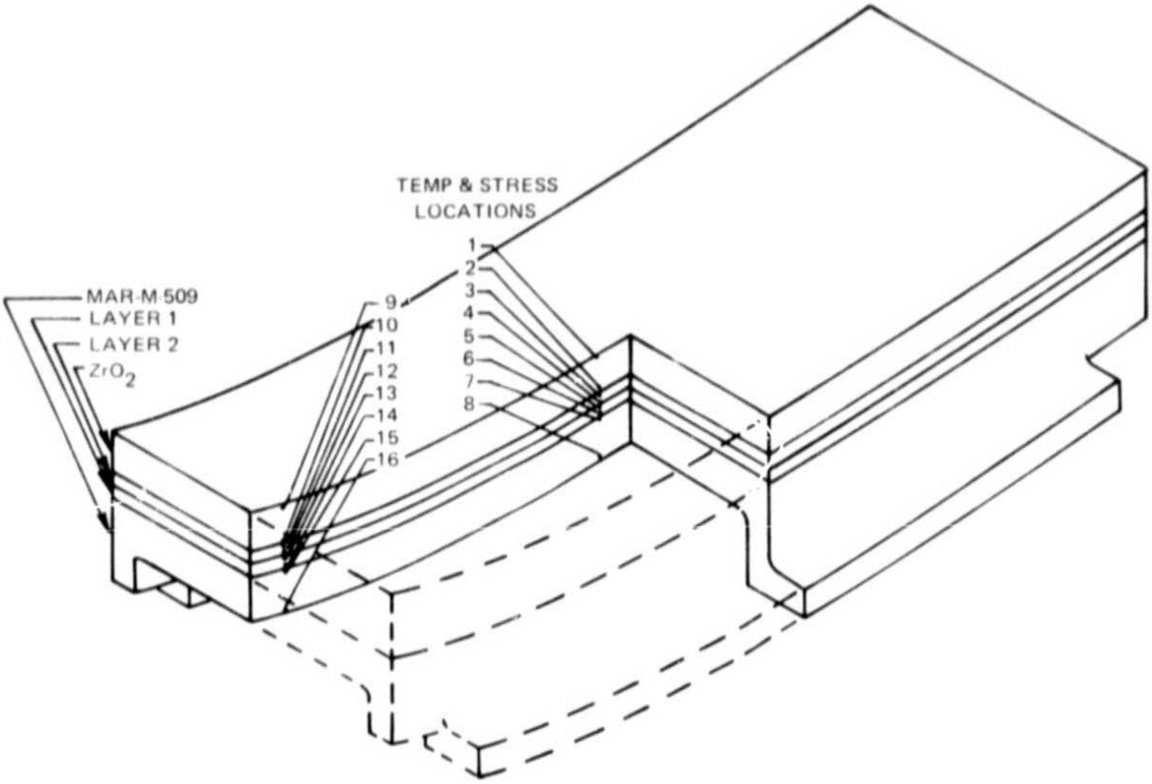

Figure 8 Material Optimization Study Specimen Configuration

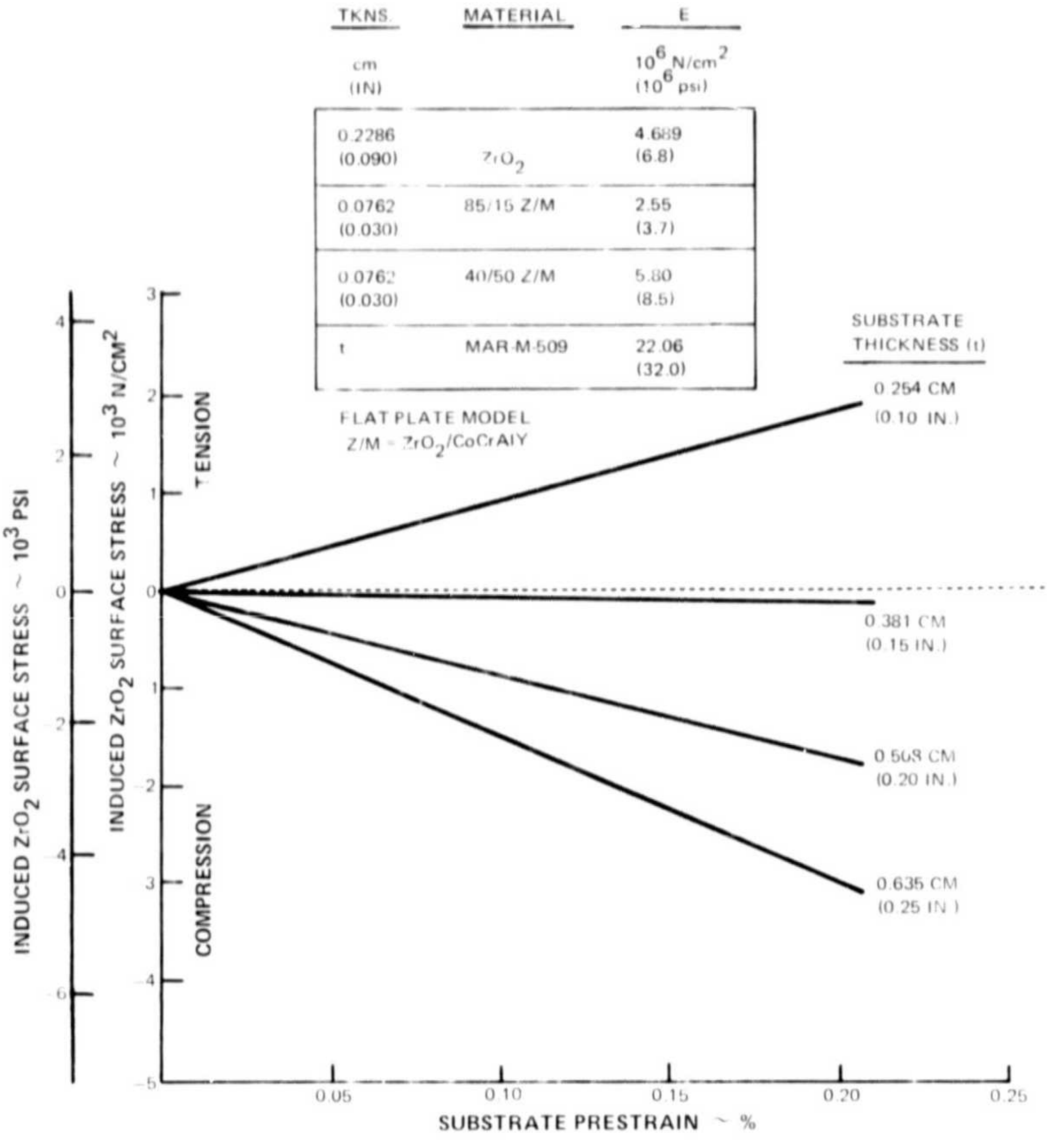

Figure 9 Estimated Stress Induced at ZrO_2 Surface by Tensile Prestraining Substrate

TKNS cm (IN)	MATERIAL	E 10^6 N/cm^2 (10^6 psi)
0.2286 (0.090)	ZrO_2	4.684 (6.8)
0.0762 (0.030)	85/15 Z/M	2.55 (3.7)
0.0762 (0.030)	40/60 Z/M	5.80 (8.5)
t	MAR-M-509	22.06 (32.0)

FLAT PLATE MODEL
Z/M = ZrO_2/CoCrAlY

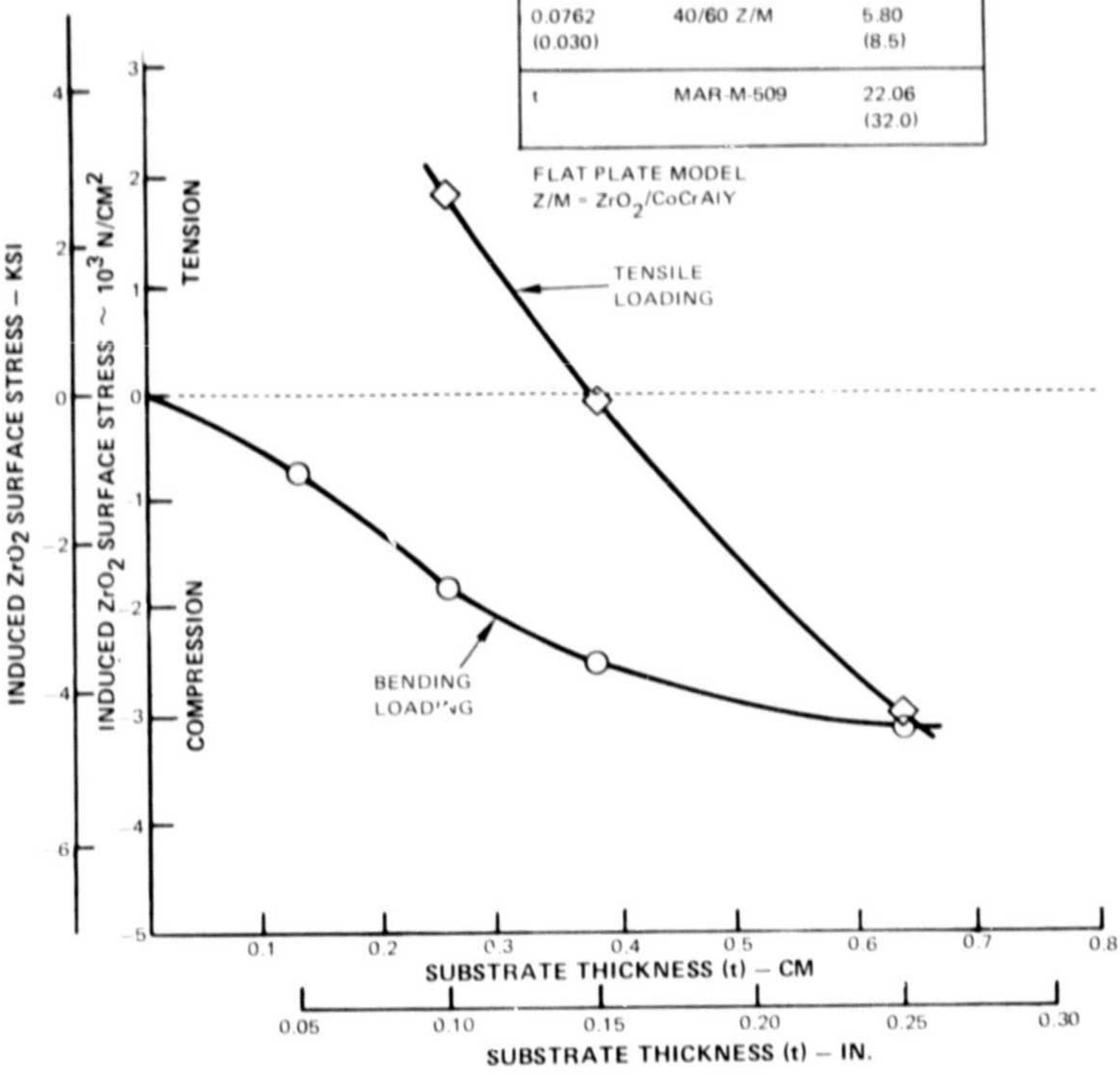

Figure 10 Estimated Stress Induced at ZrO_2 Surface by Mechanically Prestressing Substrate to 80% Yield Strength in Two Mutually Perpendicular Planes Parallel to Seal Surface

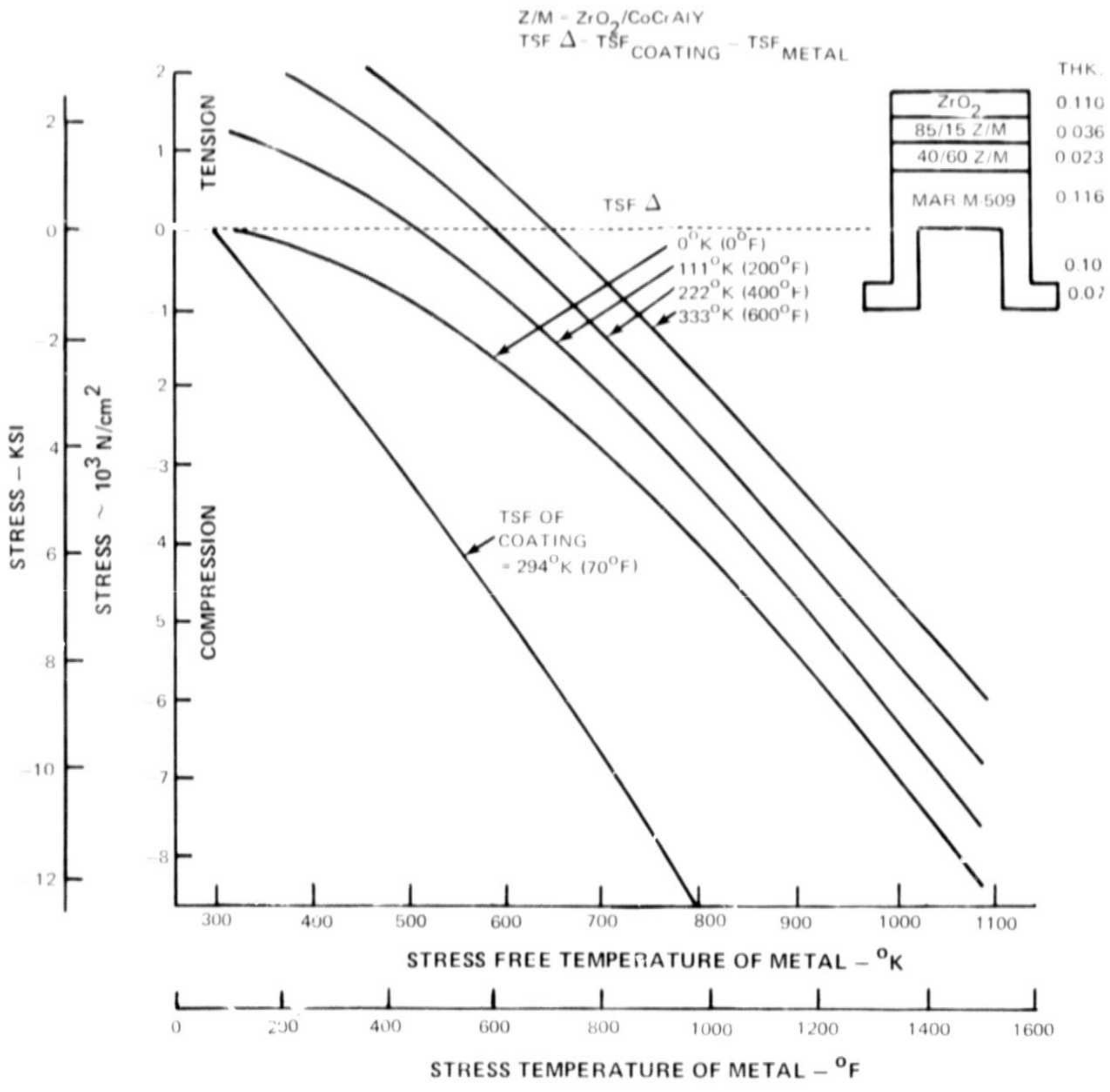

Figure 11 Estimated Stress Free Temperature Effect on Residual Stress in Rub Specimen at ZrO_2 Surface

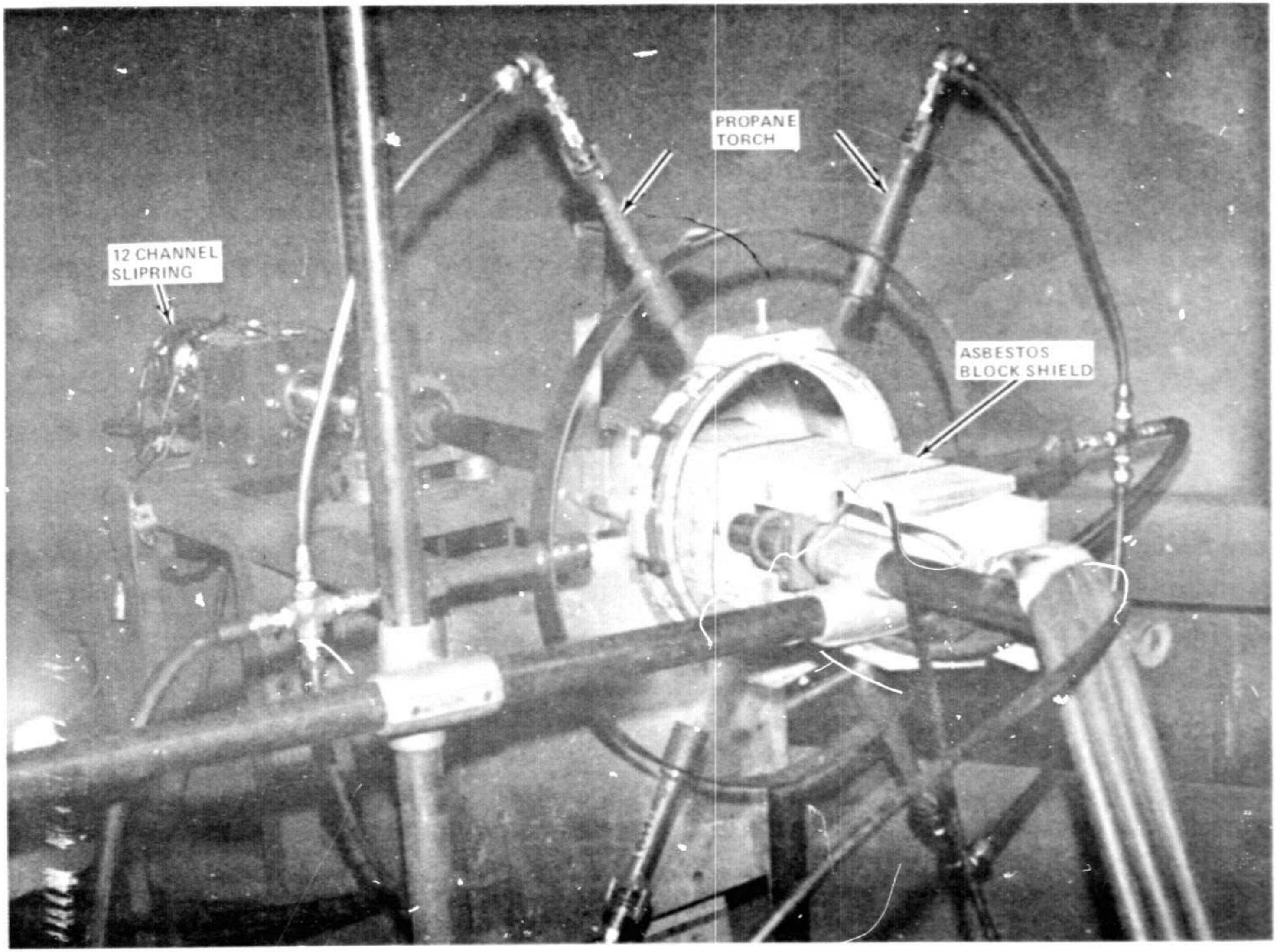

Figure 12 Equipment Used to Heat Parts During Spraying

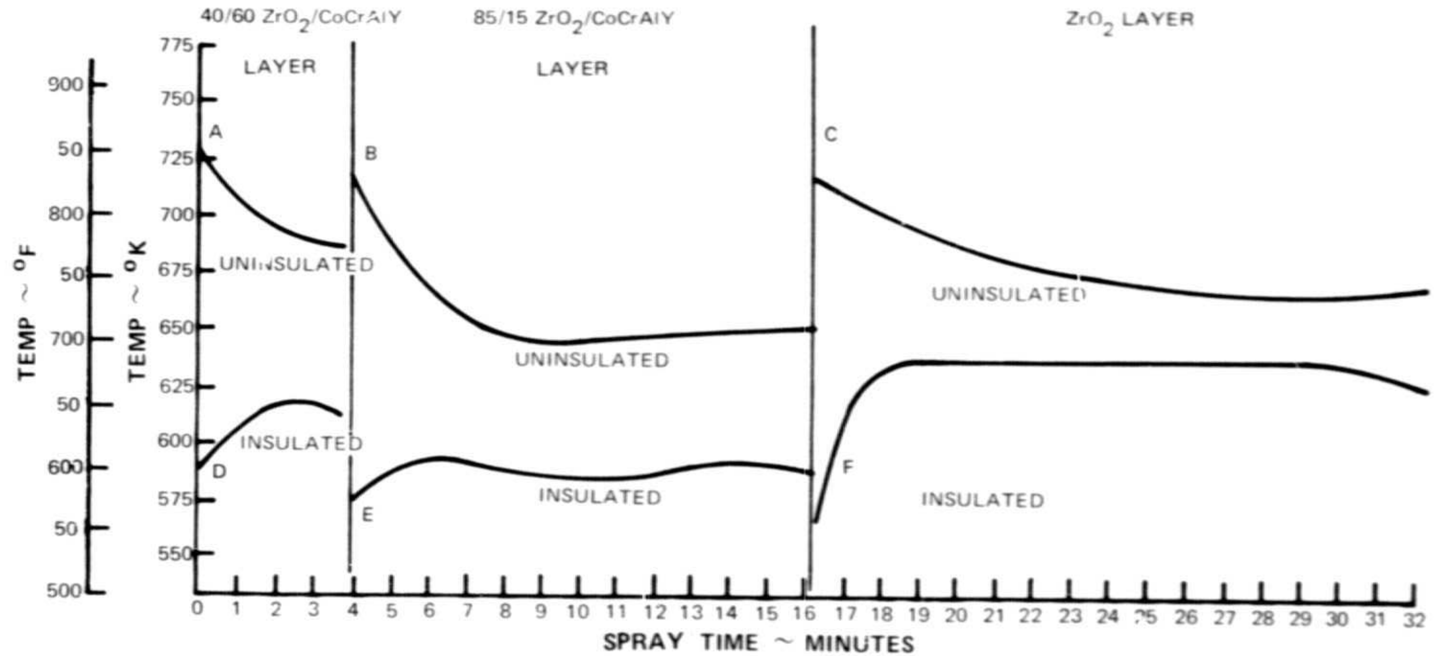

Figure 13 Specimen Substrate Temperature Versus Spray Time

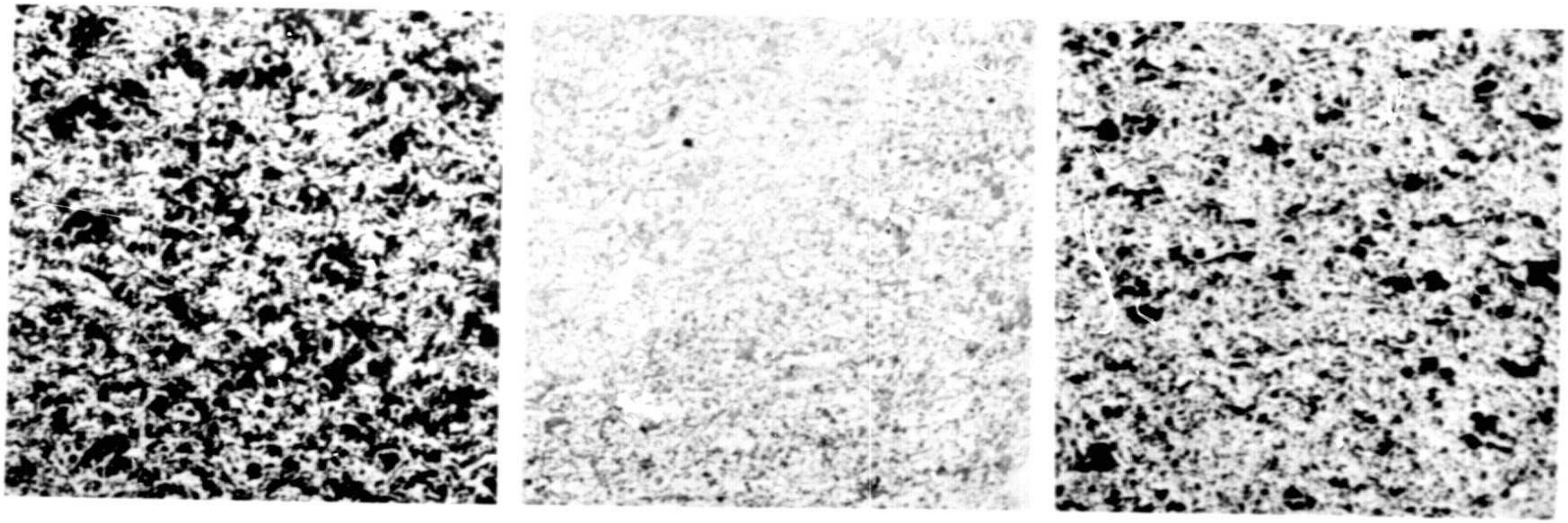

NAS3-19759 BASELINE WITHOUT SUPPLEMENTARY HEATING

589°K (600°F) SUBSTRATE

723°K (850°F) SUBSTRATE

MAG 100X

Figure 14   Microstructural Comparison of Heated Specimens With NAS3-19759 Final Configuration – ZrO_2 Layer (77-441-9898-I)

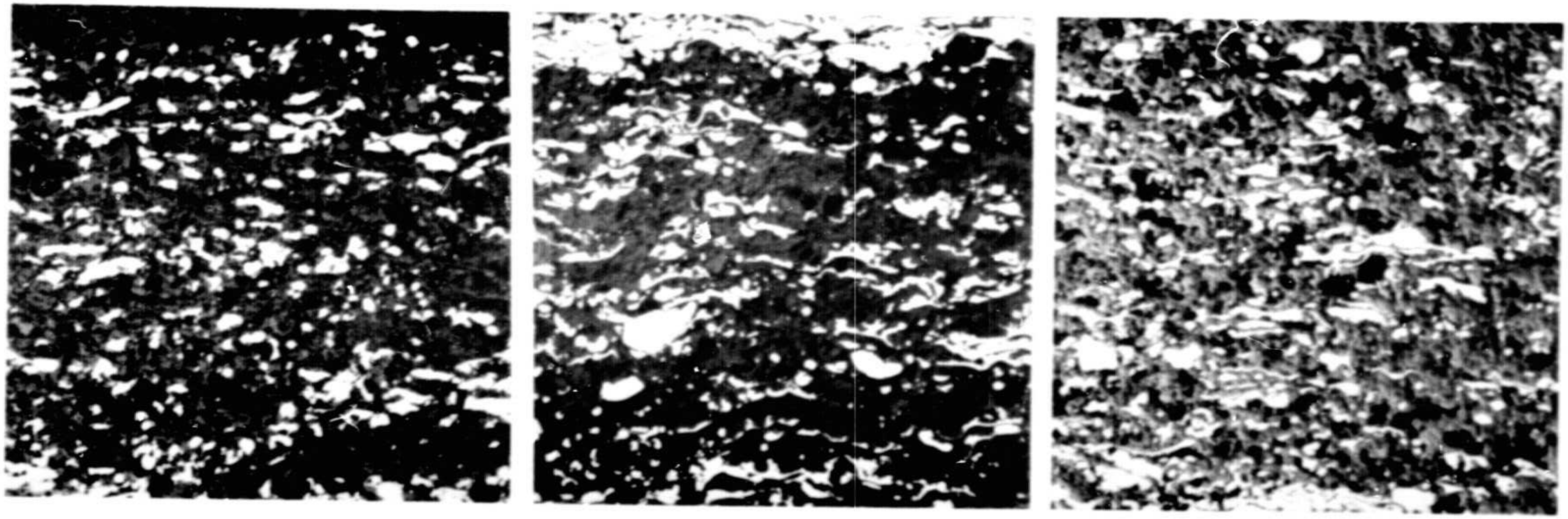

NAS3-19759 BASELINE
WITHOUT SUPPLEMENTARY HEATING

589°K (600°F) SUBSTRATE

728°K (850°F) SUBSTRATE

MAG 100X

Figure 15 Microstructural Comparison of Heated Specimens With NAS3-19759 Final Configuration – 85/15 ZrO_2/CoCrAlY Layer (77-441-9898-J)

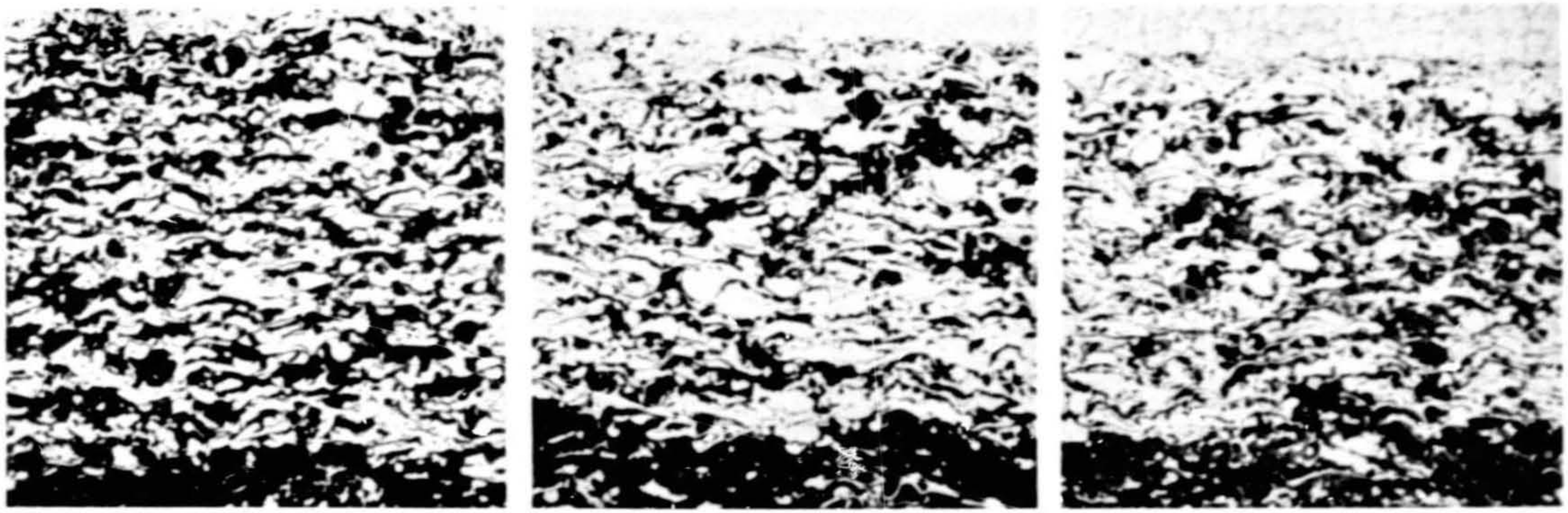

NAS3-19759 BASELINE WITHOUT SUPPLEMENTARY HEATING

589°K (600°F) SUBSTRATE

728°K (850°F) SUBSTRATE

MAG 100X

Figure 16 Microstructural Comparison of Heated Specimens With NAS3-19759 Final Configuration - 40/60 ZrO_2/CoCrAlY (77-441-9898-K)

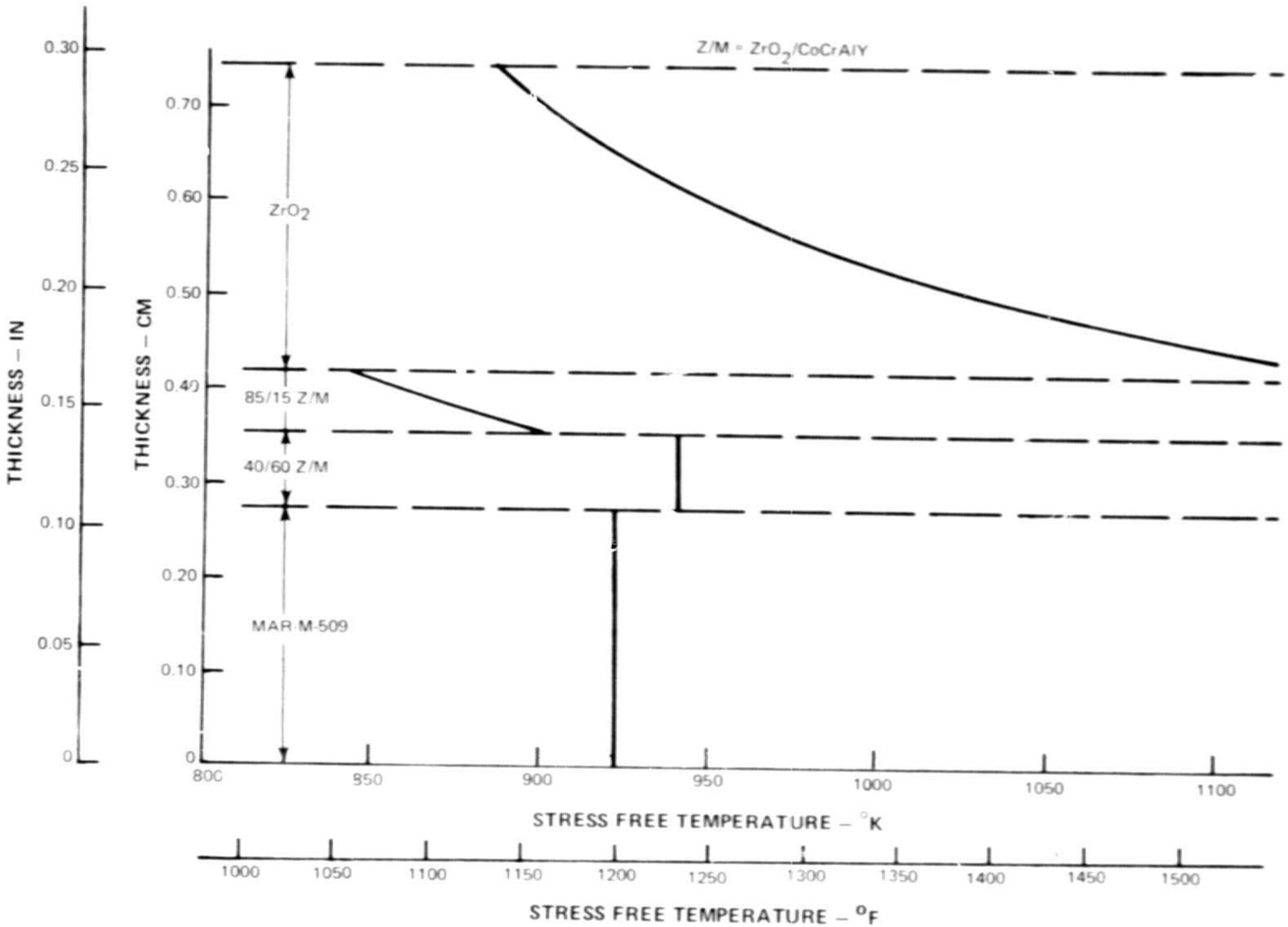

Figure 17   922°K (1200°F) Residual Stress Specimen Stress Free Temperature Versus Thickness   NAS3-19759 Material Properties

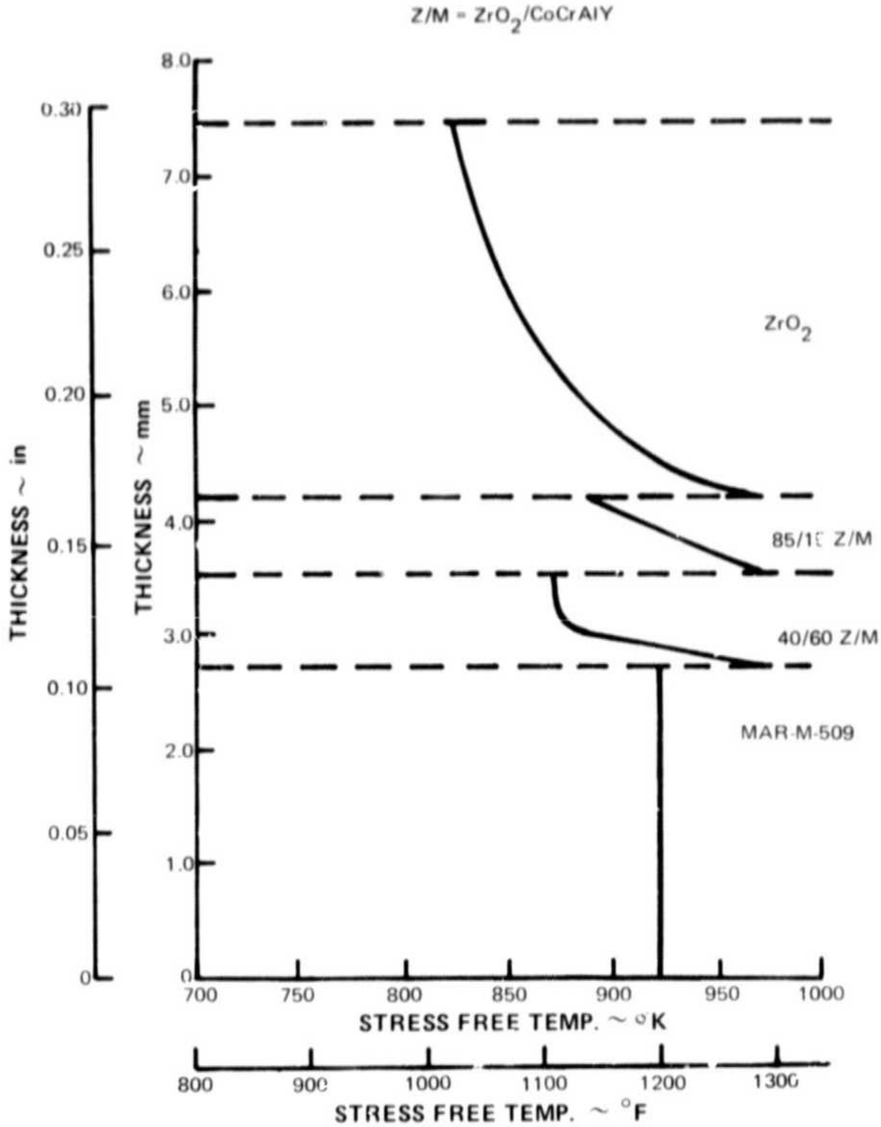

Figure 18 Stress Free Temperature Distribution, 922°K (1200°F) Seal System – 922°K (1200°F) Material Properties

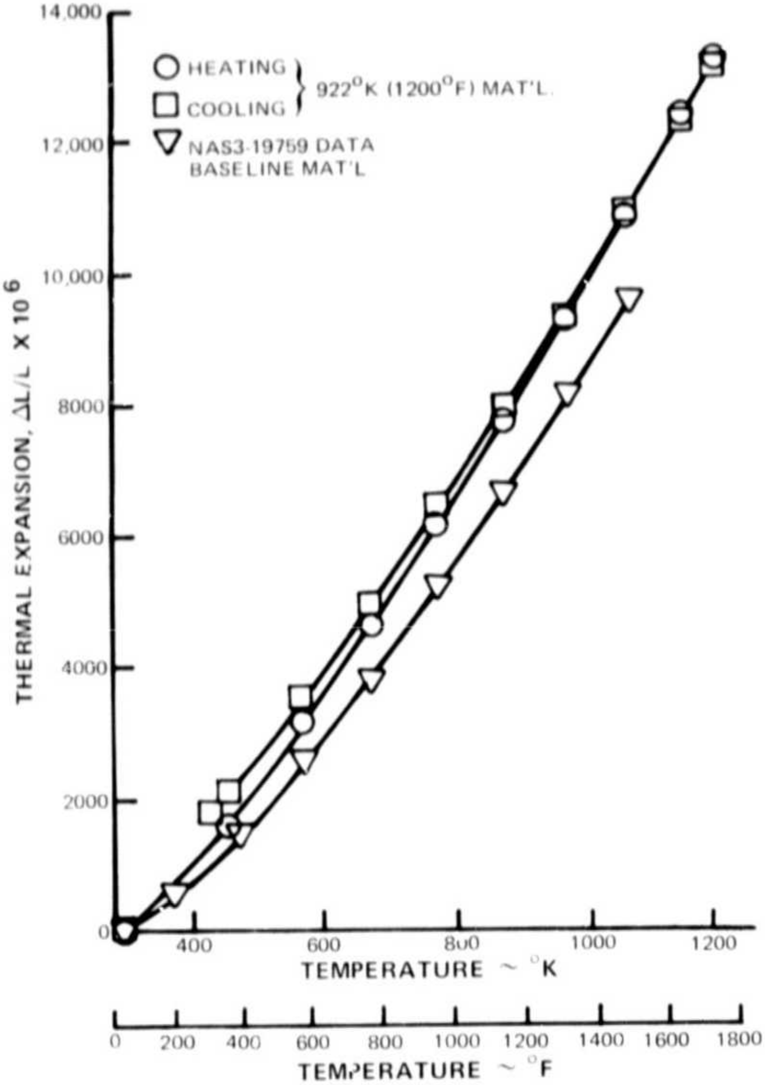

Figure 19 Thermal Expansivity, Plasma Sprayed 40/60 ZrO_2/CoCrAlY

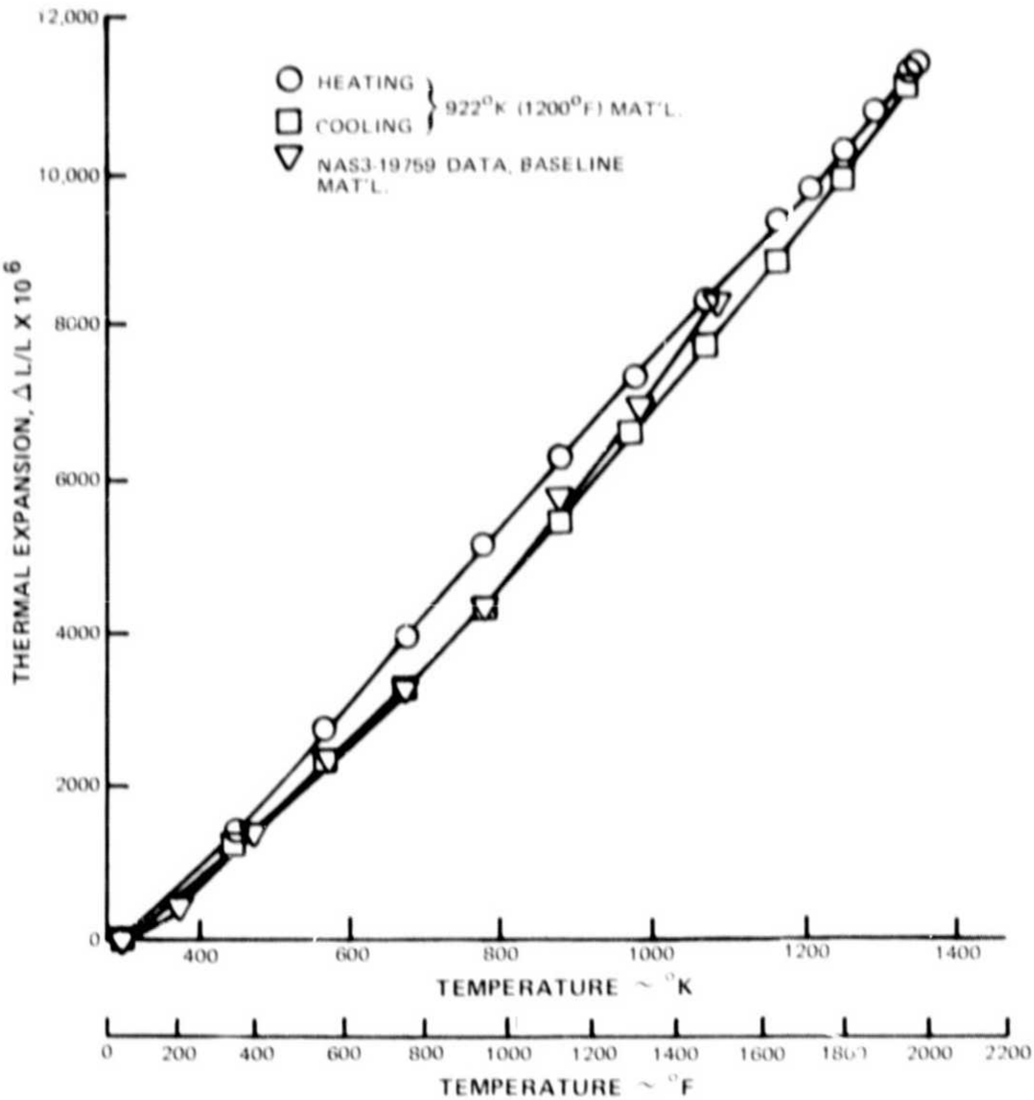

Figure 20 Thermal Expansivity, Plasma Sprayed 85/15 ZrO_2/CoCrAlY

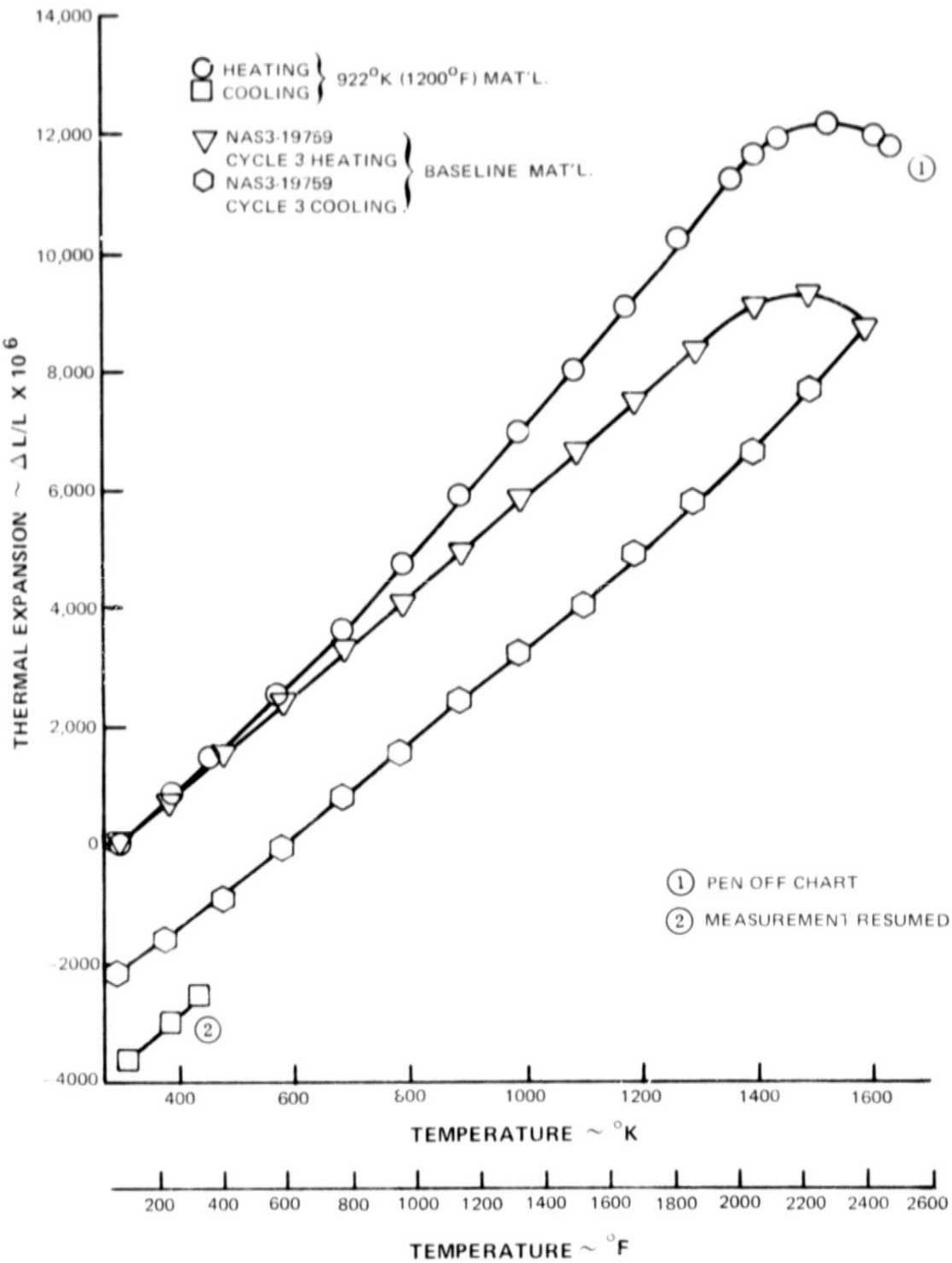

Figure 21 Thermal Expansivity, Plasma Sprayed ZrO_2 - First Cycle

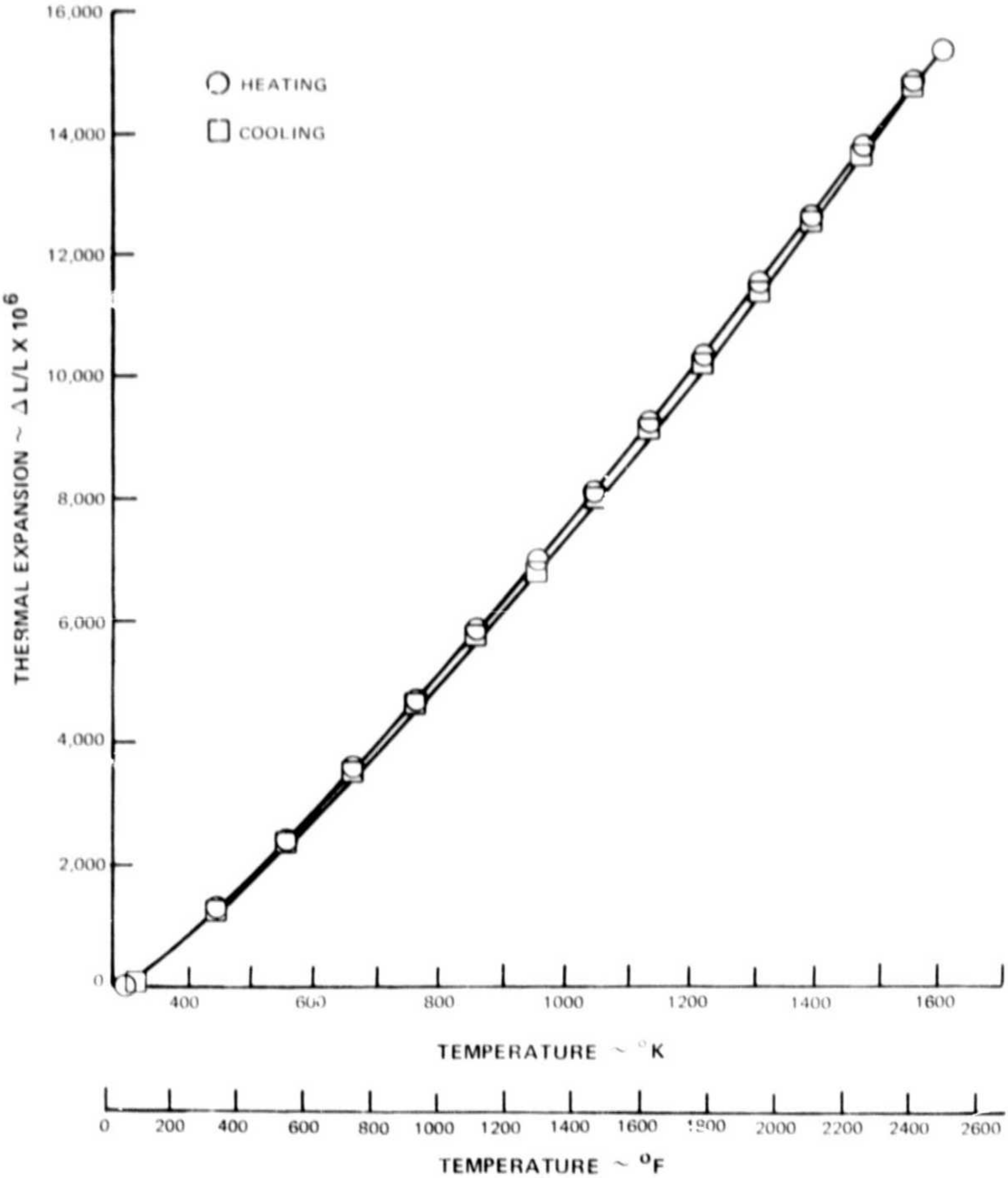

Figure 22 Thermal Expansivity, Plasma Sprayed ZrO_2 on 922°K (1200°F) Metal Substrate - Second Cycle

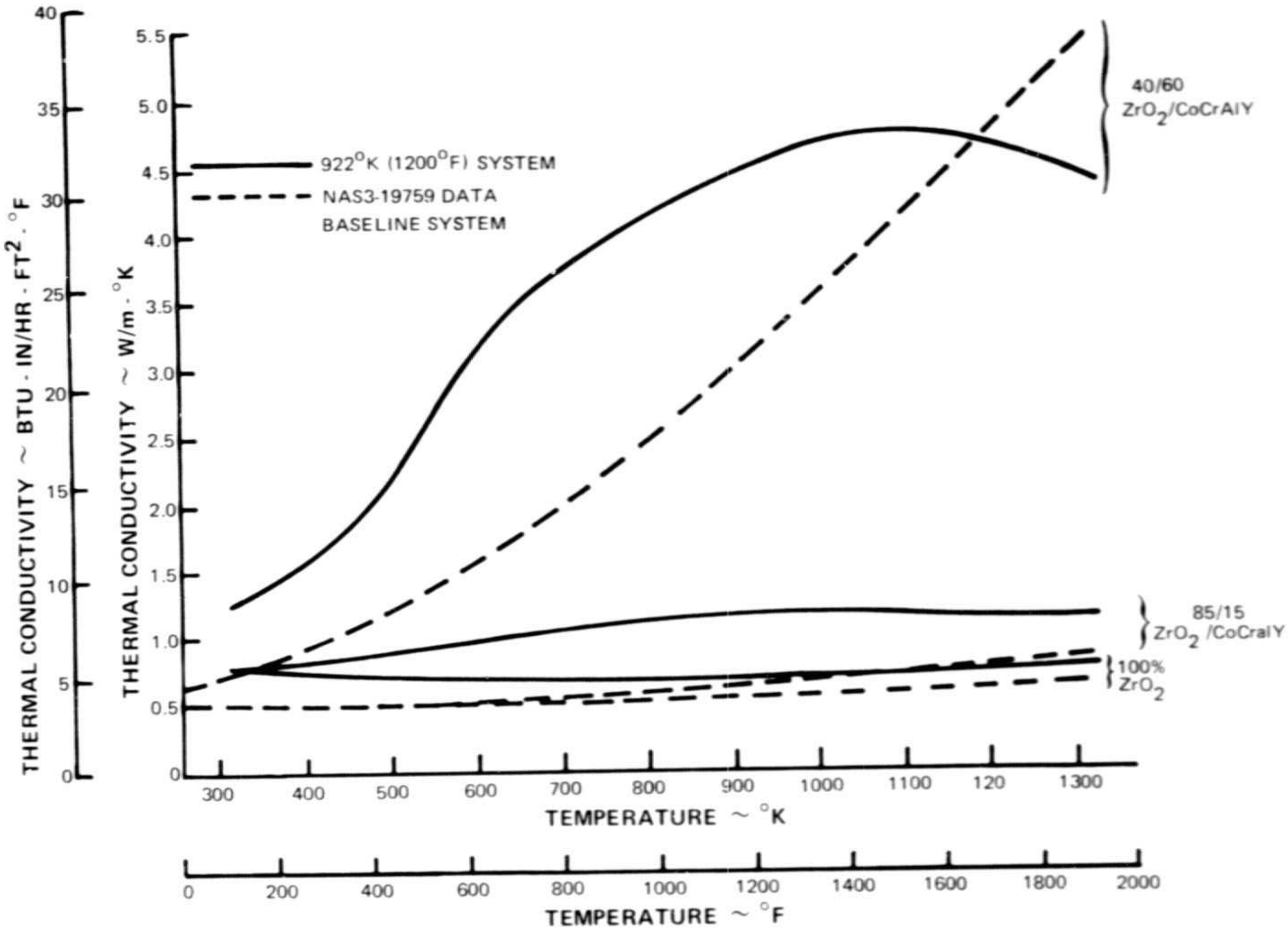

Figure 23 Thermal Conductivity Versus Temperature

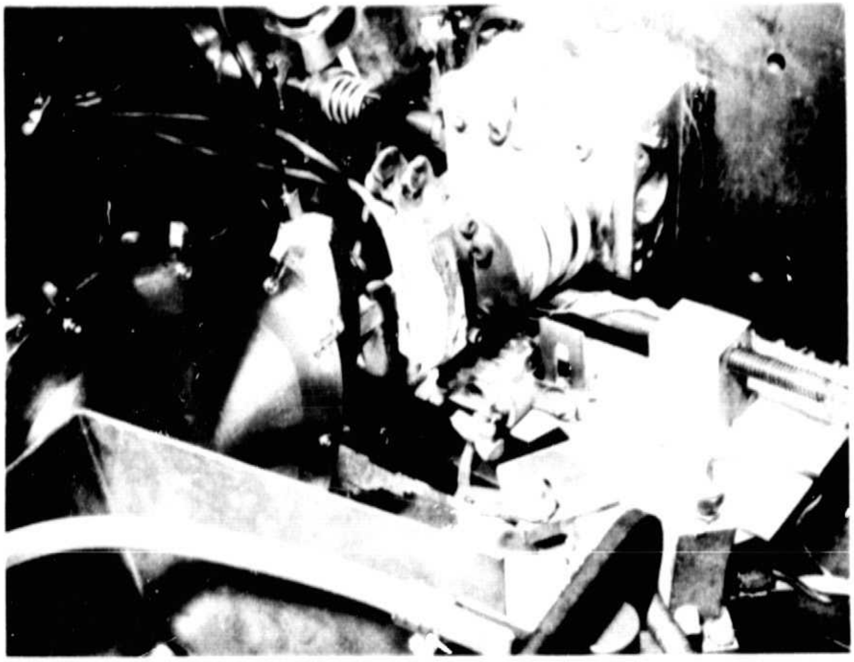

Figure 24 High Temperature Abradability Test Rig (PWA-5521)

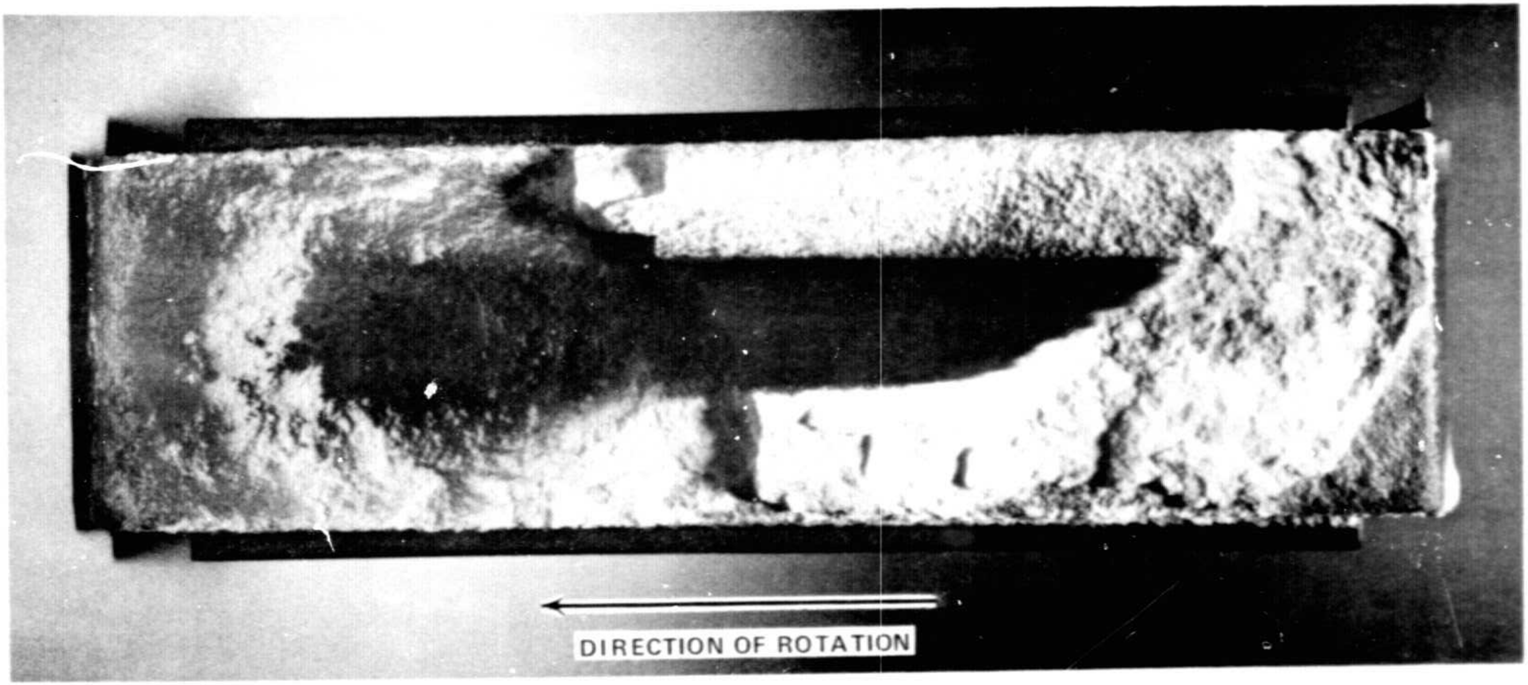

Figure 25 Abradability Test Specimen No. 3, 922°K (1200°F) Seal System (78-441-8013-A)

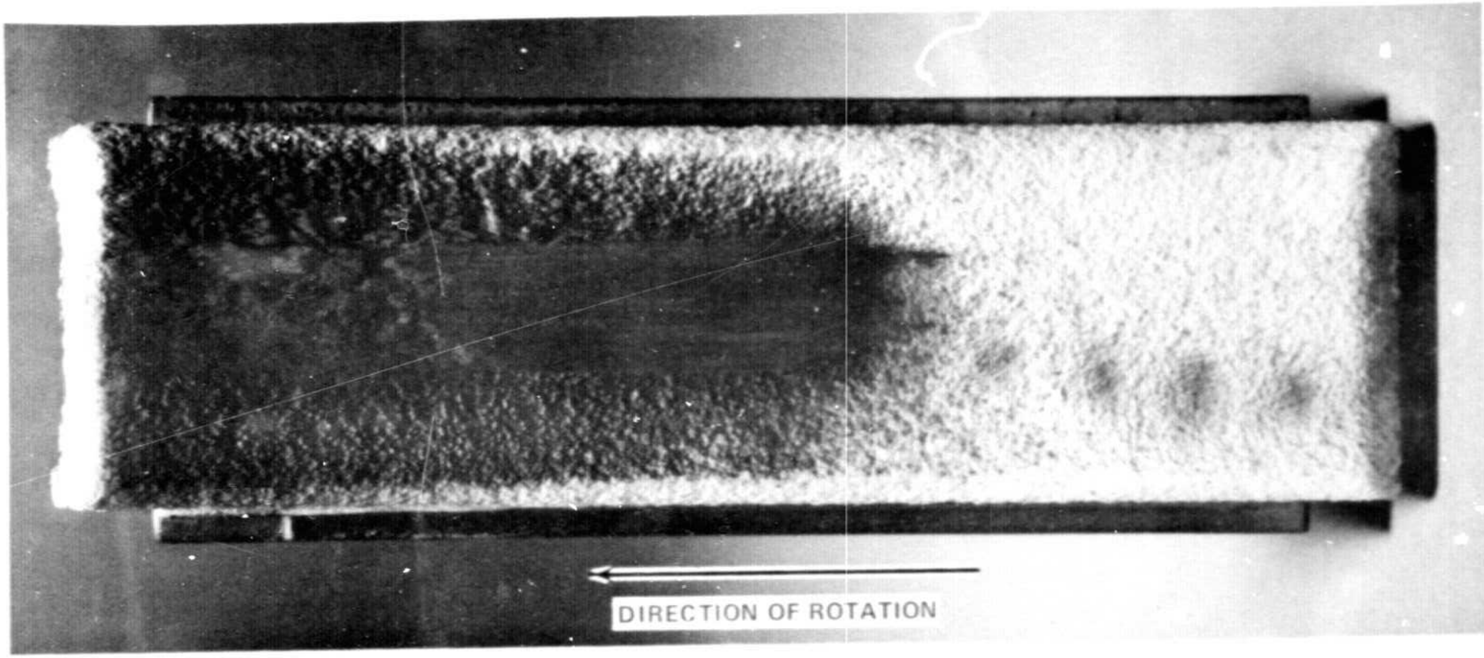

Figure 26 *Abradability Test Specimen No. 4, 922°K (1200°F) Seal System (78-441-8013 C)*

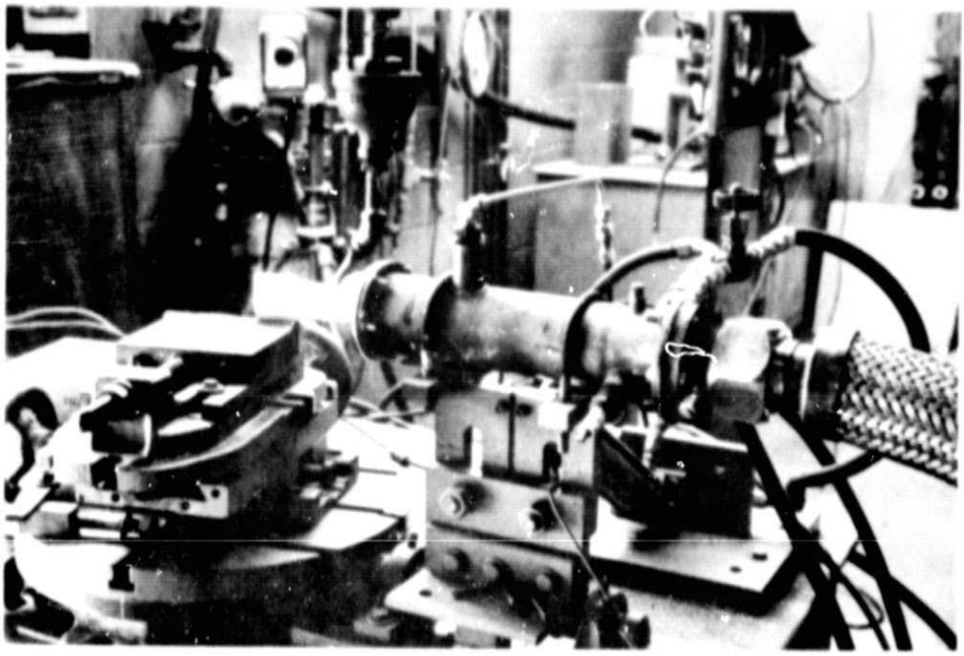

Figure 27   Hot Particulate Erosion Rig

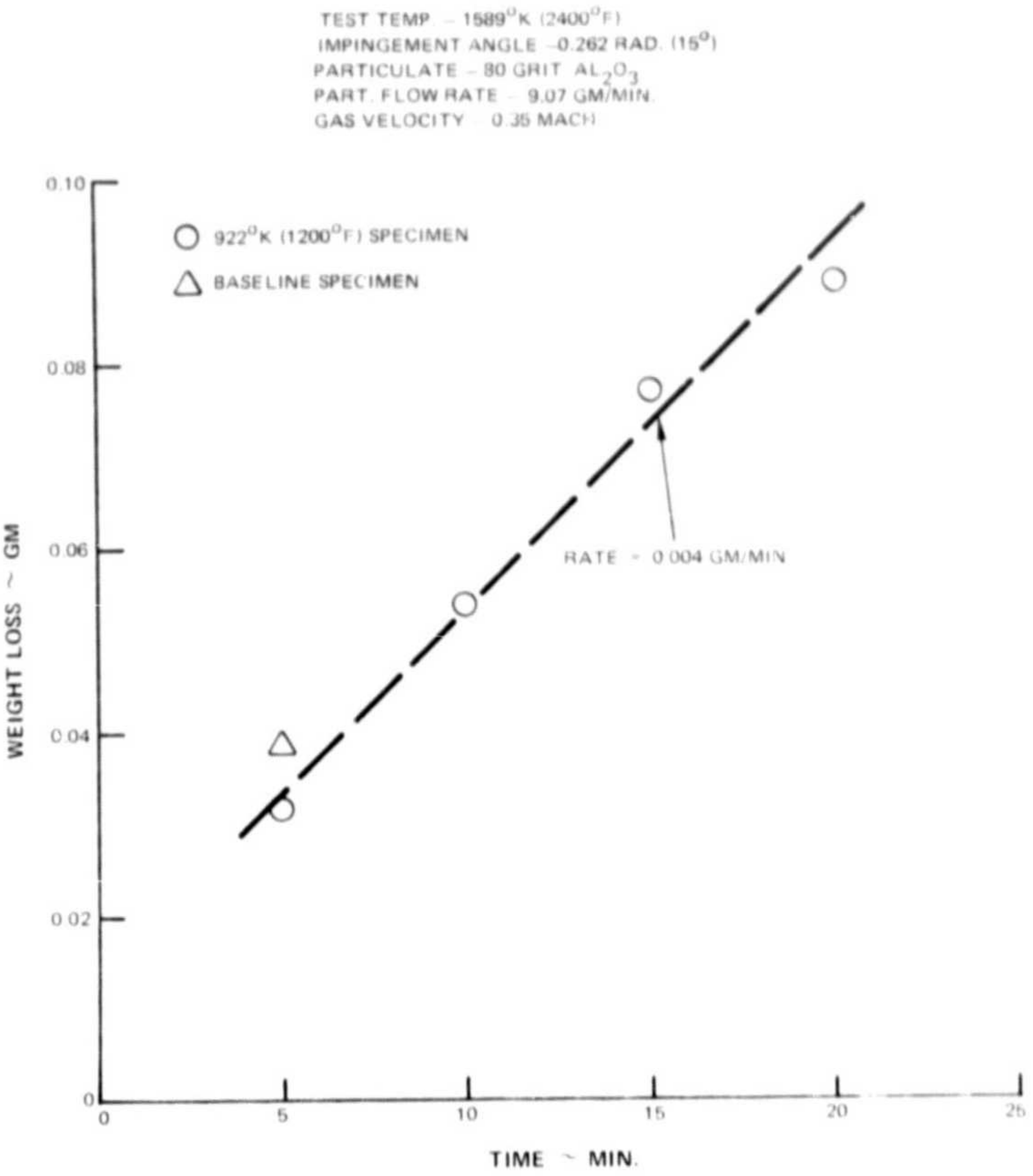

Figure 28 Erosion Test Results

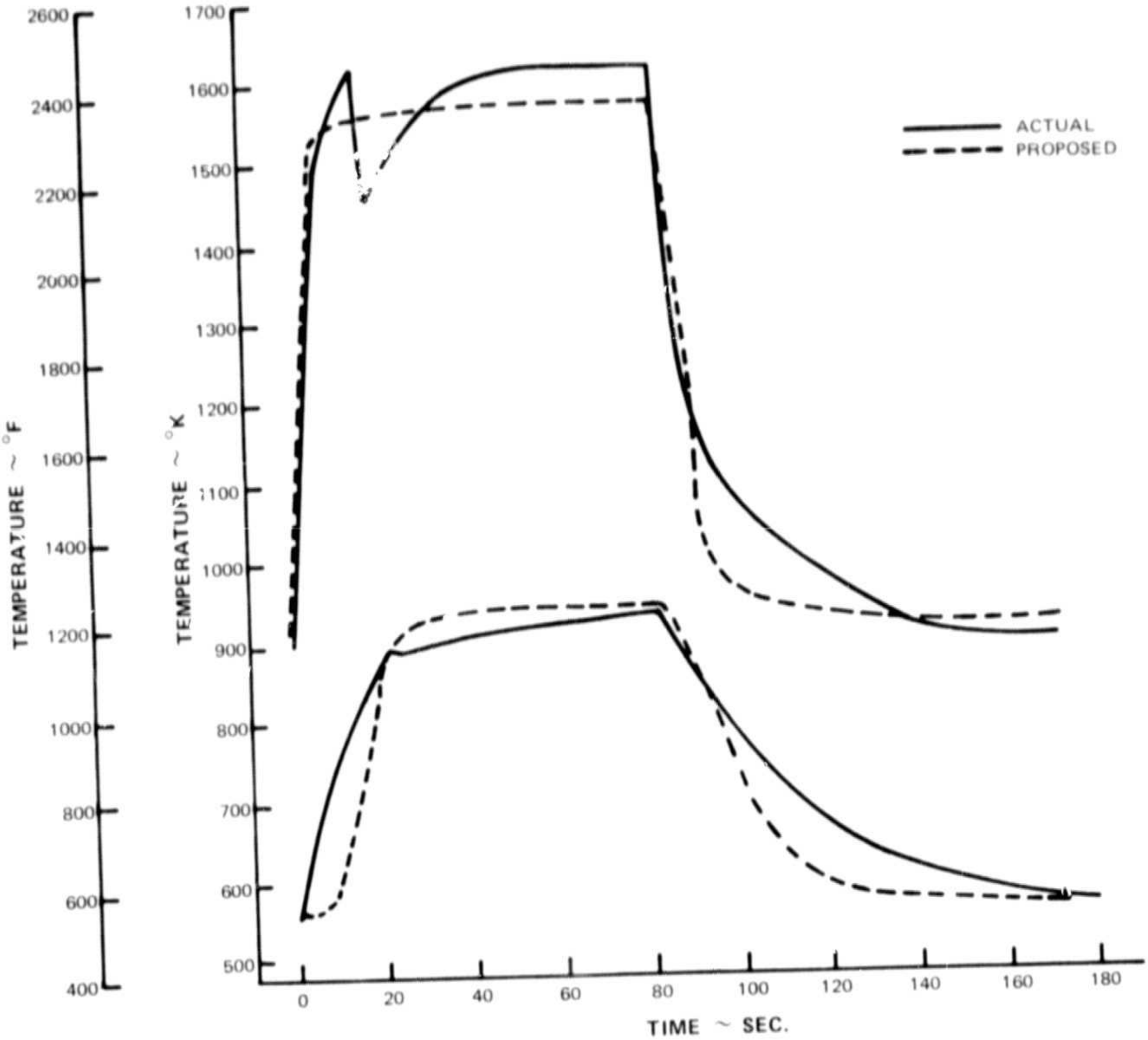

Figure 29 Thermal Fatigue Test Cycle

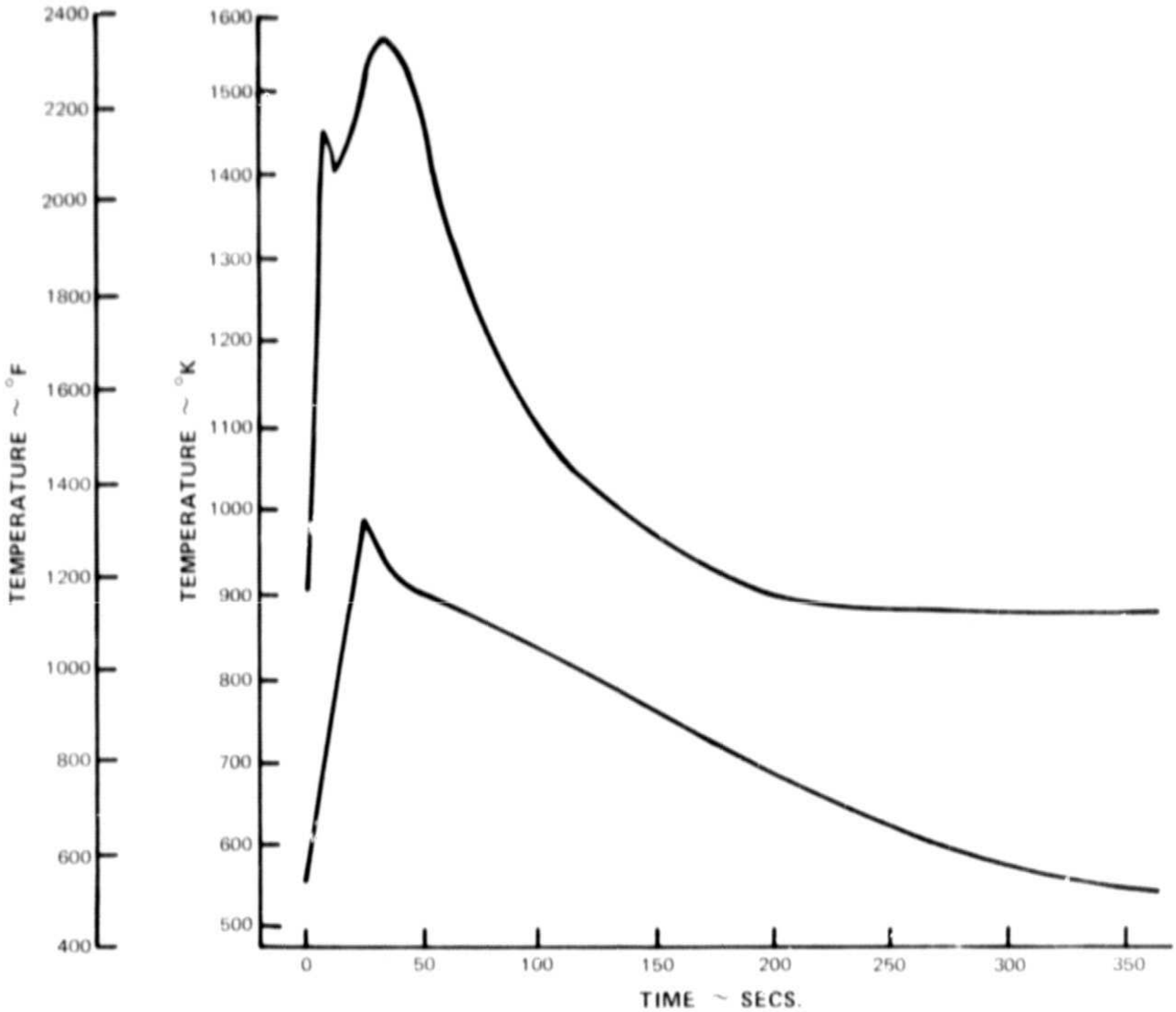

Figure 30 Initial Acceleration Heatup Cycle

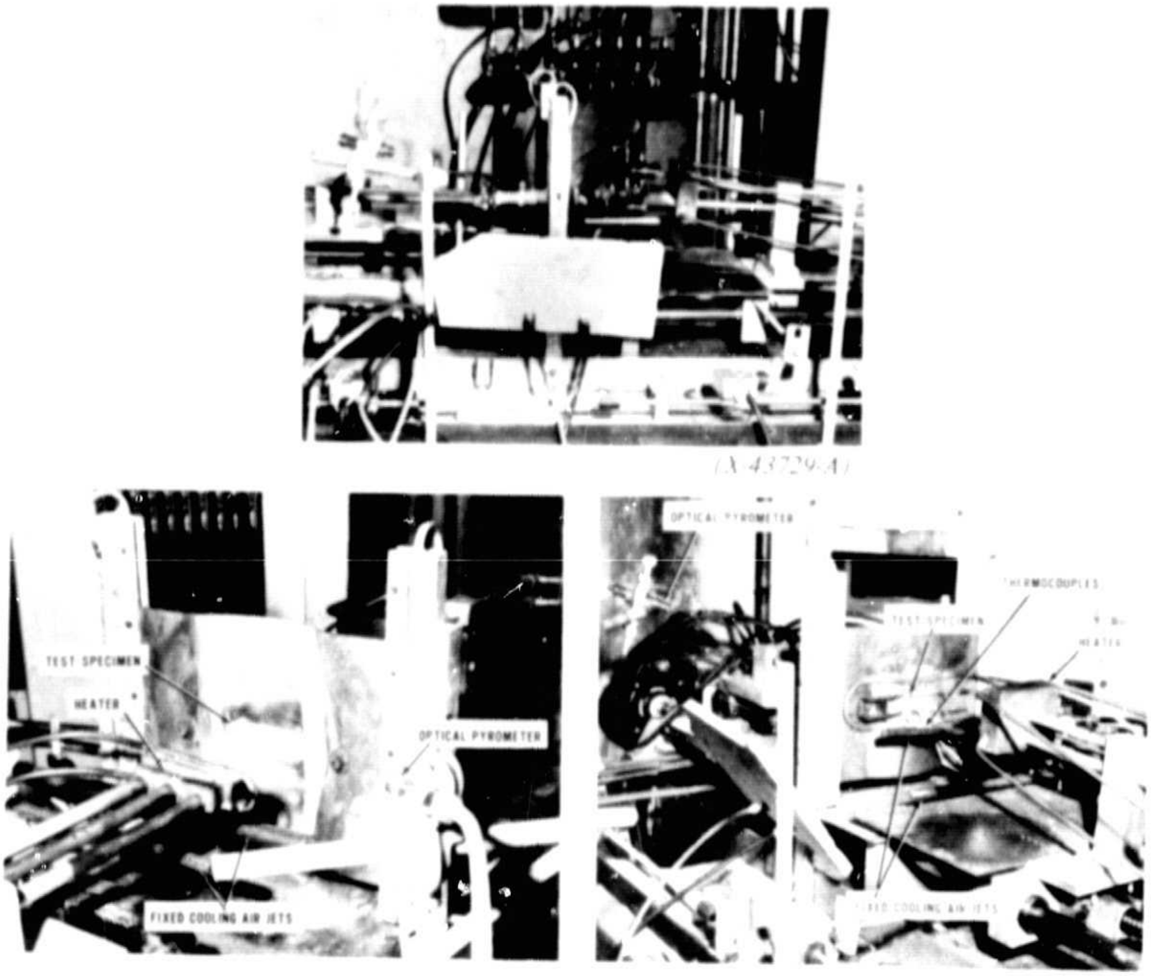

(X-43729-A)

(X-43732-A)

(X-43731-A)

Figure 31 Thermal Fatigue Test Rig

Thermal Cycle:
Max. Temp.: Surface - 1622°K (2460°F); Back - 933°K (1220°F)
Min. Temp.: Surface - 895°K (1151°F); Back - 553°K (535°F)
Max. Gradient: 794°K (1430°F) @ 16 sec
Cycle Duration: Heating - 83 sec.; cooling - 106 sec.
No. Cycles: 500

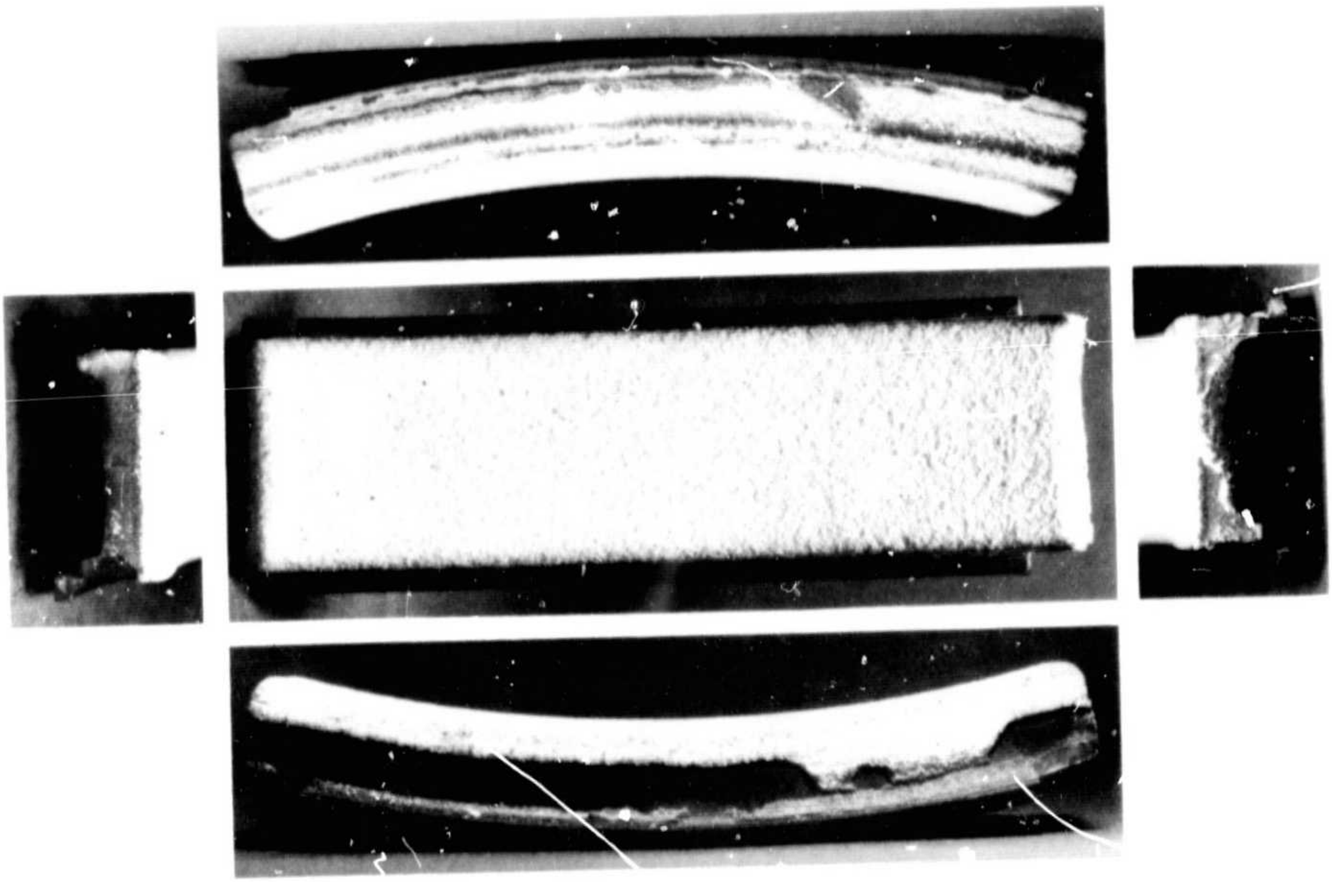

Figure 32 Thermal Fatigue Specimen (Test No. 1) Baseline Seal System (78-441-8086)

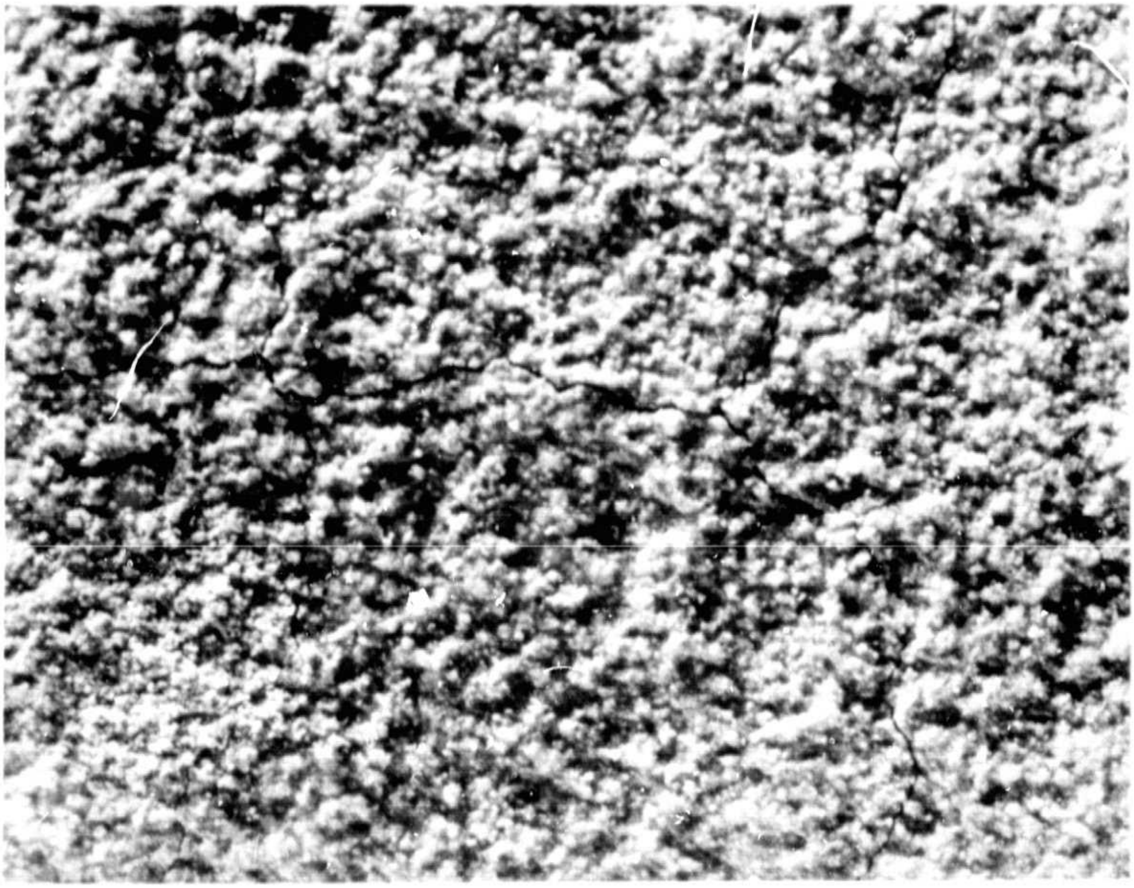

Figure 33 Radial (Mud Flat) Cracks – Thermal Fatigue Test No. 1 Baseline Seal System (77-441-0995-L)

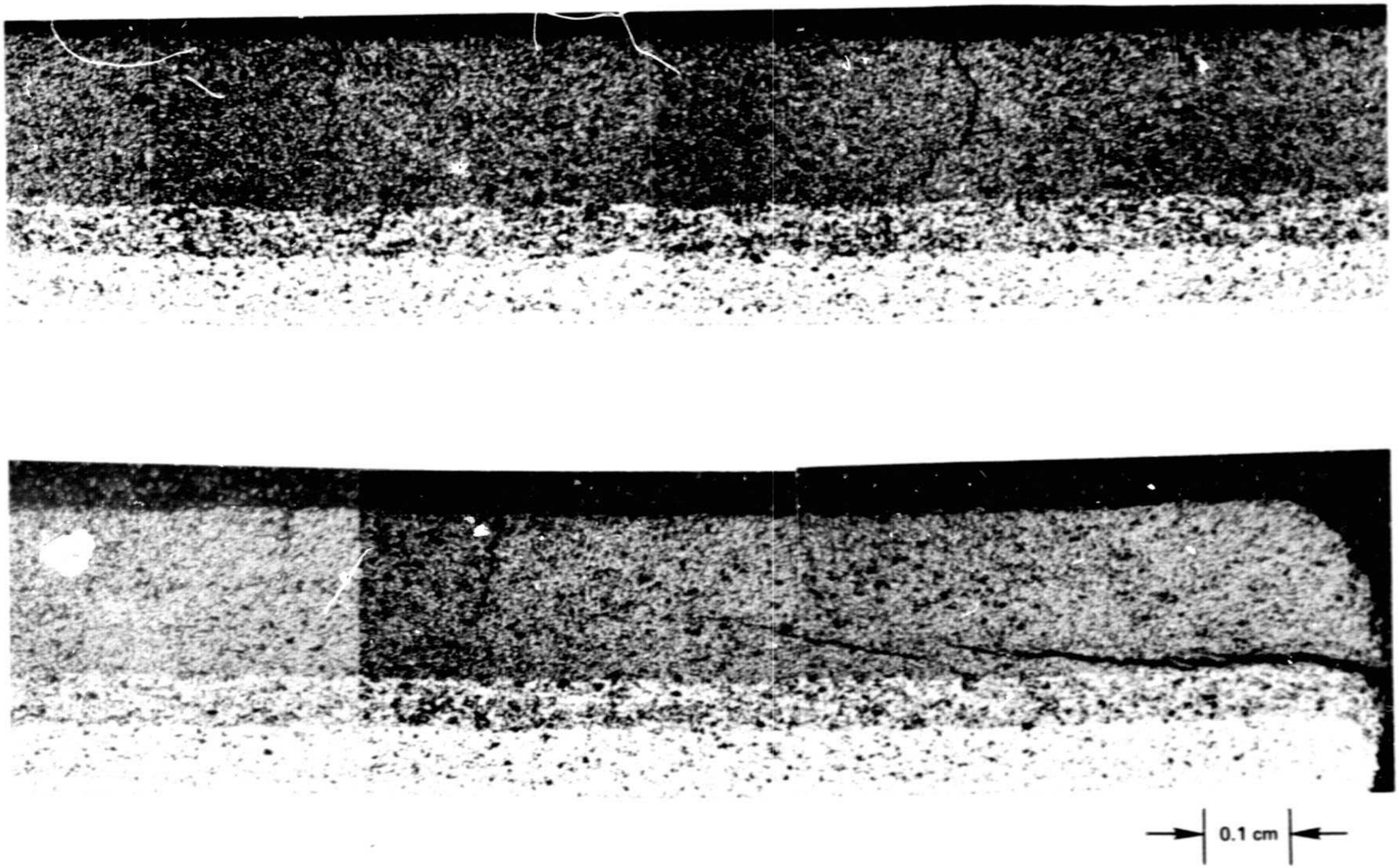

Figure 34   Circumferential Section Through Thermal Fatigue Specimen No. 1 (78-441-8415)

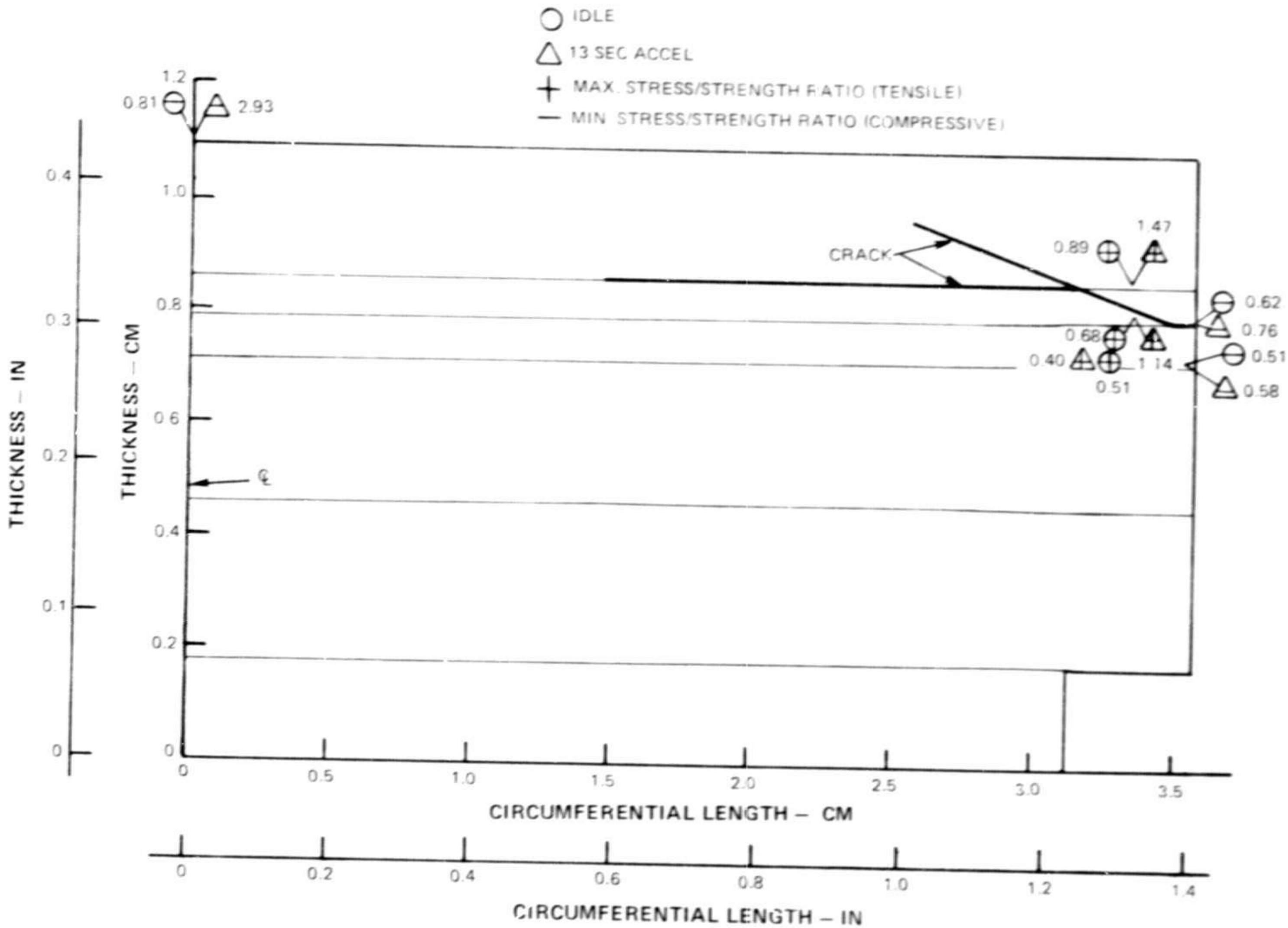

Figure 35 *922°K (1200°F) Specimen Initial Idle and Initial Acceleration Test Cycles Maximum and Minimum Principal Stress Map*

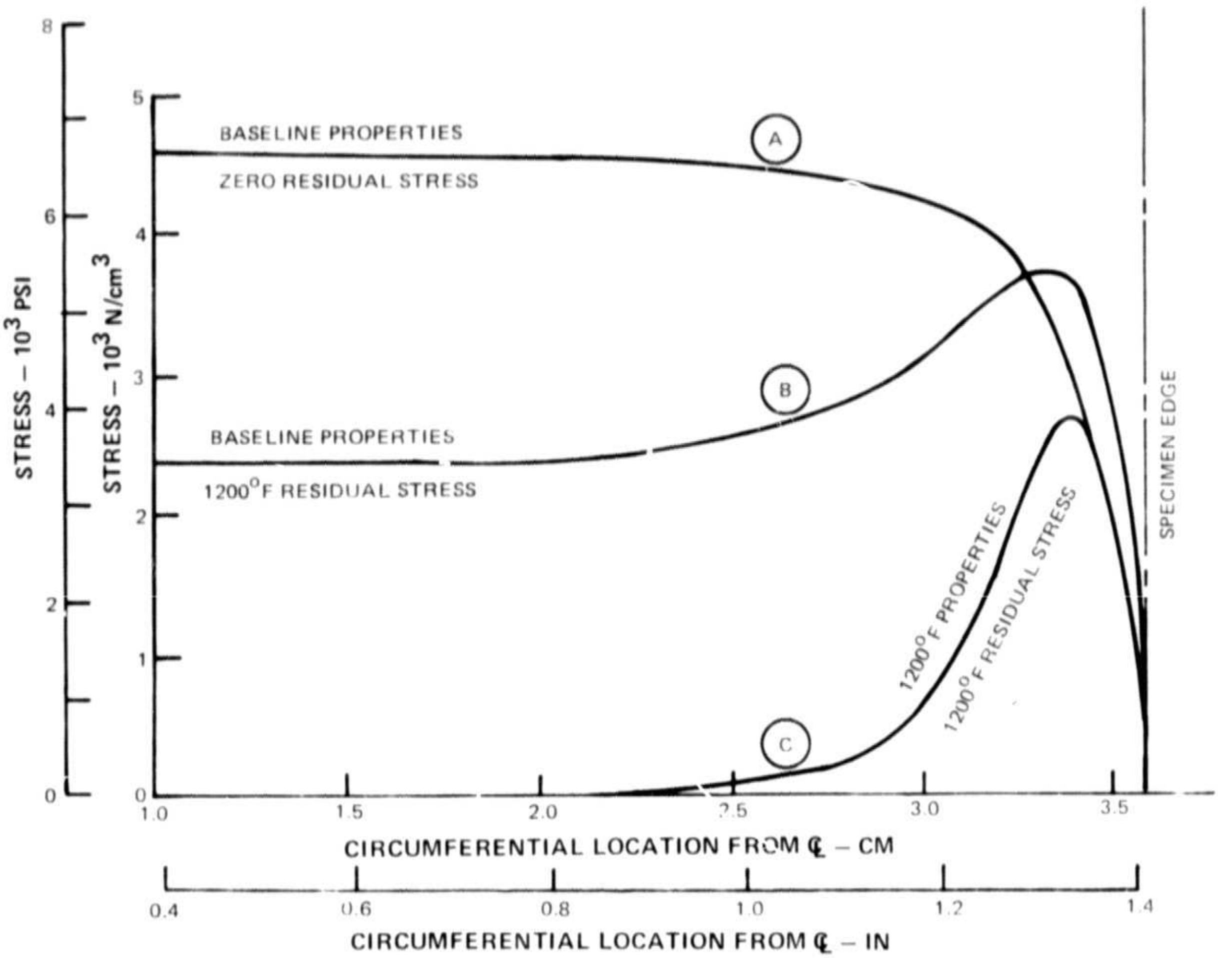

Figure 36 Calculated Maximum Principal Stress Near ZrO_2 Layer Interface for SLTO Conditions

TABLE I

MATERIAL OPTIMIZATION STUDY RESULTS AT CENTER

Z/M = ZrO_2/CoCrAlY
T = Temperature, °K (°F)

σ = Circumferential Stress, N/cm^2 (psi)

Neg. sign (-) = compression

Variation	Material Layer 1	Material Layer 2	Cycle Point	Parameter	Location 1	2	3	4	5	6	7	8
			SLTO	σ	-3119	4054	1042	3212	9272	11435	-8564	-6159
					(-4524)	(5879)	(1511)	(4658)	(13448)	(16585)	(-12420)	(-8933)
				T	1542	1170	1092	1020	975	960	951	946
Baseline	40/60 Z/M	85/15 Z/M			(2315)	(1646)	(1506)	(1376)	(1295)	(1268)	(1252)	(1242)
				σ	-11477	2748	2504	3357	9736	9812	5156	3251
			6 sec Accel		(-16645)	(3985)	(3631)	(4869)	(14121)	(14231)	(7478)	(4715)
				T	1352	661	614	579	563	561	562	566
					(1973)	(729)	(645)	(582)	(553)	(549)	(552)	(559)
			SLTO	σ	-2105	5459	2169	4332	831	1528	-5914	-5224
					(-3053)	(7918)	(3146)	(6283)	(1205)	(2216)	(-8578)	(-7576)
				T	1540	1156	1076	1000	959	955	952	947
1	10/90 Z/M	85/15 Z/M			(2312)	(1620)	(1476)	(1340)	(1266)	(1259)	(1253)	(1244)
				σ	-12285	2528	2470	3356	9309	9675	6323	6003
					(-17817)	(3667)	(3582)	(4867)	(13501)	(14032)	(7171)	(8706)
			6 sec Accel	T	1350	647	601	568	558	558	559	564
					(1970)	(705)	(622)	(563)	(544)	(544)	(546)	(555)
				σ	-2641	7858	1360	2467	8266	10495	-10743	-8978
			SLTO		(-3831)	(11396)	(1973)	(3578)	(11988)	(15221)	(-15596)	(-13021)
2	40/60 Z/M	30/70 Z/M		T	1529	1061	1004	997	985	967	957	951
					(2292)	(1450)	(1348)	(1335)	(1313)	(1281)	(1262)	(1251)
				σ	-12587	3474	7057	7888	8074	8653	2920	3333
			6 sec Accel		(-18255)	(5039)	(10235)	(11440)	(11710)	(12549)	(4235)	(4834)
				T	1346	609	578	574	568	564	564	568
					(1963)	(636)	(580)	(573)	(563)	(556)	(556)	(563)
				σ	-2886	4069	1127	3370	6068	6129	-5225	-4089
			SLTO		(-4186)	(5898)	(1634)	(4887)	(8800)	(8889)	(-7621)	(-6974)
				T	1541	1162	1080	1001	958	954	951	946
3	10/90 Z/M	90/10 Z/M			(2313)	(1631)	(1484)	(1342)	(1265)	(1258)	(1252)	(1243)
				σ	12331	2466	3012	4068	9109	9494	6129	5851
			6 sec Accel		(17884)	(3476)	(4368)	(5900)	(13211)	(13769)	(8889)	(8486)
				T	1350	648	601	568	558	558	559	564
					(1970)	(706)	(622)	(563)	(544)	(544)	(546)	(555)

TABLE II

MATERIAL OPTIMIZATION STUDY RESULTS NEAR END

Z/M = ZrO_2/CoCrAlY
T = Temperature, °K (°F)

σ = Circumferential Stress, N/cm^2 (psi)

Neg. sign (-) = compression

Variation	Material Layer 1	Material Layer 2	Cycle Point	Parameter	Location 9	10	11	12	13	14	15	16
Baseline	40/60 Z/M	85/15 Z/M	SLTO	σ	-3676 (-5332)	3614 (5241)	783 (1136)	2984 (4328)	8174 (11855)	10944 (14873)	-8296 (-12032)	-2754 (-3994)
				T	1542 (2315)	1170 (1646)	1092 (1506)	1020 (1376)	975 (1295)	960 (1268)	951 (1252)	946 (1242)
			6 sec Accel	σ	-8936 (-12960)	4502 (6529)	3303 (4791)	3929 (5698)	10669 (15474)	9736 (14120)	1729 (2508)	-9292 (-13477)
				T	1352 (1973)	661 (729)	614 (645)	579 (582)	563 (553)	561 (549)	562 (552)	566 (559)
1	10/90 Z/M	85/15 Z/M	SLTO	σ	-3030 (-4394)	4803 (6966)	1804 (2616)	4049 (5872)	-941 (-1365)	1073 (1556)	-4782 (-6935)	-176 (-255)
				T	1540 (2312)	1156 (1620)	1076 (1476)	1000 (1340)	959 (1266)	955 (1259)	952 (1253)	947 (1244)
			6 sec Accel	σ	-9226 (-13381)	4722 (6848)	3459 (5017)	4051 (5875)	11741 (17029)	8912 (12926)	1375 (1994)	-8830 (-12806)
				T	1350 (1970)	647 (705)	601 (622)	568 (563)	558 (544)	558 (544)	559 (546)	564 (555)
2	40/60 Z/M	30/70 Z/M	SLTO	σ	-3725 (-5402)	6952 (10083)	-1670 (-2422)	519 (744)	7562 (10968)	10639 (15430)	-4747 (-12686)	-2063 (-2992)
				T	1529 (2292)	1061 (1450)	1004 (1348)	997 (1335)	985 (1313)	967 (1281)	957 (1262)	951 (1251)
			6 sec Accel	σ	-10176 (-14759)	5012 (7269)	9615 (13945)	9101 (13199)	8142 (11809)	8090 (11733)	-1100 (-1596)	-8773 (-12724)
				T	1346 (1963)	609 (636)	578 (580)	574 (573)	568 (563)	564 (556)	564 (556)	568 (563)
3	10/90 Z/M	90/10 Z/M	SLTO	σ	-3363 (-4878)	3645 (5287)	884 (1282)	3174 (4604)	5907 (8567)	6085 (8825)	-5158 (-7481)	-2490 (-3612)
				T	1541 (2313)	1162 (1631)	1080 (1484)	1001 (1342)	958 (1265)	954 (1258)	951 (1252)	946 (1243)
			6 sec Accel	σ	-9319 (-13515)	4639 (6728)	4213 (6110)	4895 (7100)	11360 (16476)	8638 (12528)	1156 (1677)	-8835 (-12813)
				T	1350 (1970)	648 (706)	601 (622)	568 (563)	558 (544)	558 (544)	559 (546)	564 (555)

TABLE III

RESIDUAL STRAIN DATA
THERMAL PRESTRESSED SPECIMEN, 728°K (850°F)
Z/M = ZrO_2/CoCrAlY

Increment			Thickness	ΔStrain, 10^{-6} cm/cm	
No.	Thickness cm (in)	Material	°K (°F)	Circ.	Axial
1	0.0457 (0.018)	ZrO_2	303 (85)	45	-25
2	0.0508 (0.020)	ZrO_2	303 (85)	25	30
3	0.0508 (0.020)	ZrO_2	303 (86)	10	40
4	0.0508 (0.020)	ZrO_2	304 (87)	5	35
5	0.0508 (0.020)	ZrO_2	303 (86)	0	40
6	0.0305 (0.012)	ZrO_2	303 (86)	30	40
7	0.0279 (0.011)	85/15 Z/M	299 (78	40	--
8	0.0305 (0.012)	85/15 Z/M	301 (82)	40	--
9	0.0330 (0.013)	85/15 Z/M	302 (85)	30	--
10	0.0254 (0.010)	40/60 Z/M	299 (79)	10	--
11	0.0305 (0.012)	40/60 Z/M	300 (80)	25	--
12	0.0152 (0.006)	40/60 Z/M	300 (80)	-10	--
13	0.0254 (0.010)	Mar-M-509	286 (55)	60	--
14	0.0254 (0.010)	Mar-M-509	297 (65)	25	--

TABLE IV

RESIDUAL STRESS SPECIMENS
CURVATURE CHANGE

	Substrate Radius, cm (in)		
	Before Spraying	After Spraying	Change
922°K (1200°F) System	14.295 (5.628)	15.100 (5.945)	+0.805 (+0.317)
	12.896 (5.077)	13.830 (5.445)	+0.934 (+0.368)
Baseline System	12.649 (4.980)	12.761 (5.024)	+0.112 (+0.044)
	13.597 (5.353)	13.884 (5.466)	+0.287 (+0.113)

TABLE V

RESIDUAL STRAIN MEASUREMENTS
922°K (1200°F) THERMAL TREATED SPECIMEN

Increment No.	Material	Thickness, mm (in)	Strain Change, 10^{-6} cm/cm Circ.	Axial	Diagonal	Remarks
1	ZrO_2	0.762 (0.030)	10	20	20	
2	ZrO_2	0.762 (0.030)	50	26	30	
3	ZrO_2	0.762 (0.030)	90	54	80	
4	ZrO_2	0.635 (0.025)	100	80	80	
5	ZrO_2	0.356 (0.014)	50	80	70	
6	85/15 Z/M	0.406 (0.016)	140	110	140	
7	85/15 Z/M	0.254 (0.010)	80	60	70	
8	40/60 Z/M	0.330 (0.013)	120	0	30	
9	40/60 Z/M	0.203 (0.008)	80	10	70	
10	40/60 Z/M	0.279 (0.011)	50	-50	0	
Residual	Mar-M-509	2.718 (0.107)	--	--	--	Assumed Stress Free at 922°K (1200°F) For Analysis

Z/M = ZrO_2/CoCrAlY
C = Circumferential Strain Gage
A = Axial Strain Gage
D = Diagonal Strain Gage

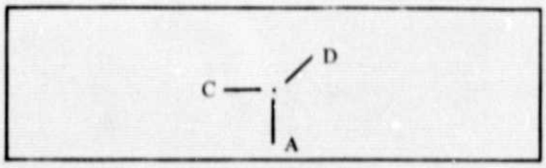

Gage Orientation

TABLE VI

AVERAGE MODULII OF RUPTURE AND ELASTICITY
AND STRAIN TO FAILURE TEST RESULTS FOR
MATERIALS SPRAYED ON 922°K (1200°F) METAL SUBSTRATE

Material	Test Temperature °K	(°F)	Modulus of Rupture 10^3 N/cm²	(10^3 psi)	Modulus of Elasticity 10^6 N/cm²	(10^6 psi)	Strain To Failure, %
40/60 ZrO_2/CoCrAlY	293	(68)	10.14	(14.7)	7.10	(10.30)	0.206
	1256	(1800)	7.45	(10.8)	4.28	(6.21)	0.537
85/15 ZrO_2/CoCrAlY	293	(68)	3.64	(5.28)	5.57	(8.08)	0.101
	1256	(1800)	5.33	(7.73)	3.68	(5.33)	0.292
ZrO_2	293	(68)	1.83	(2.66)	2.50	(3.63)	0.107
	1589	(2400)	2.36	(3.42)	2.39	(3.47)	0.345

TABLE VII

AVERAGE MODULII OF RUPTURE AND ELASTICITY AND STRAIN TO FAILURE TEST RESULTS FOR MATERIALS SPRAYED WITHOUT SUPPLEMENTAL HEATING OF METAL SUBSTRATE

Material	Test Temperature °K	(°F)	Modulus of Rupture 10^3 N/cm²	(10^3 psi)	Modulus of Elasticity 10^6 N/cm²	(10^6 psi)	Strain To Failure, %
40/60 ZrO_2/CoCrAlY	293	(68)	22.27	(32.3)	5.86	(8.5)	0.82
	1005	(1350)	10.83	(15.7)	9.24	(13.4)	0.39
70/30 ZrO_2/CoCrAlY	293	(68)	5.63	(8.16)	3.62	(5.25)	0.43
	1061	(1450)	7.03	(10.2)	4.70	(6.81)	0.47
85/15 ZrO_2/CoCrAlY	293	(68)	4.14	(6.0)	2.54	(3.68)	0.40
	1144	(1600)	4.70	(6.82)	1.86	(2.70)	0.34
ZrO_2	293	(68)	2.82	(4.09)	4.69	(6.8)	0.12
	1589	(2400)	2.24	(3.32)	1.56	(2.26)	0.33

TABLE VIII

ABRADABILITY TEST RESULTS

Test No.	1	2	3	4
Description	922°K (1200°F) System Machined Surface	Baseline, As Sprayed Surface	922°K (1200°F) System As-Sprayed Surface	922°K (1200°F) System As-Sprayed Surface
Avg. Hardness, R_s45Y	86.6	74.7	78.0	76.2
No. Blades	12	12	12	12
Blade Tip Dia., cm (in)	21.49 (8.46)	21.49 (8.46)	21.49 (8.46)	21.49 (8.46)
Blade Tip Velocity, m/s (ft/sec)	204.8 (1000)	204.8 (1000)	284.4 (933)	304.8 (1000)
Seal Temp., °K (°F)	1589 (2400)	1589 (2400)	1589 (2400)	1589 (2400)
Interaction Rate, mm/s (in/sec)	---	---	0.0254 (0.001)	0.254 (0.010)*
Penetration Depth, mm (in)	---	---	0.762 (0.030)	0.762 (0.030)
Max. Seal Wear Depth, mm (in)	---	---	0.508 (0.020)	None
Transfer to Seal	---	---	Light	Heavy 0.011 in
Rub Pattern	---	---	Continuous	Continuous
Actual Surf. Temp., °K (°F)	---	---	1606 (2430)	1561 (2350)
Max. Surf. Temp., °K (°F)	---	---	1650 (2510)	1922 (3000)
Normal Load, Kg (lb)	---	---	1.814 (4)	4.989 (11)
Avg. Blade Wear, mm (in)	---	---	0.061 (0.0024)	0.980 (0.0386)
Blade Heat Discoloration	---	---	Negligible	Dark Straw
Blade Pickup	---	---	Slight on Leading Side	Up to 0.178 mm (0.007 in) on Leading Side
VWR	---	---	0.166	Indeterminate
Remarks	60% of ZrO_2 layer spalled during heatup	50% of ZrO_2 layer spalled and cracked laminarly during heatup	ZrO_2 layer partially spalled during heatup and rub, mostly outside rub path	Axial cracks in transfer. *Interaction rate slowed to 0.109 mm/s (0.0043 in/sec) during rub

TABLE IX

EROSION TEST DATA SUMMARY

Gas Velocity - 0.35 Mach
Nozzle to specimen distance - 3.81 cm (1.5 in)

Particulate: Material - Al_2O_3
Size - 80 Grit
Flow - 0.544 kg/hr (1.2 lb/hr)

Test No.	Surface Temp. °K (°F)	Impingement Angle RAD (degrees)	Avg R_s45Y	Hardness Range R_s45Y	Erosion Rate 10^{-3} gm/min	Erosion Rate 10^{-3} cc/min	Specific Erosion of Al_2O_3 10^{-4} gm/gm	Remarks
1	1589 (2400)	0.262 (15)	67.1	66.70	4.0	0.770	4.4	922°K (1200°F) system as-sprayed, eroded surface mud flat cracked
2	1589 (2400)	0.262 (15)	73.2	72-77	Undetermined			Baseline system, as-sprayed ZrO_2 layer delaminated during cool-down after 10 min.

TABLE X

THERMAL SHOCK TEST RESULTS

Test No.	Specimen	Remarks
1	Baseline system as sprayed	Completed 500 cycles. No discernible cracks until 100 cycle inspection. Surface cracks apparent after 100 cycles. "Mud flat" dimension approximately 0.51 cm (0.20 in) × 0.51 cm (0.20 in). Fine laminar cracks at both ends at ZrO_2 interface apparent after 300 cycles. Cracks extend approximately 1.27 cm (½ in) towards center. After 500 cycles, same laminar cracks extends approximately 1.9 cm (¾ in) towards center. No apparent substantial increase in surface cracking.
2	922°K (1200°F) system; machined	Severe laminar cracking at idle. Cracks occurred at both ends, apparently originting in the 85/15 ZrO_2/CoCrAlY layer and propagating into ZrO_2 layer, partially through to surface. Severe ZrO_2 surface overheating 589°K (600°F) at 6 second accel. Spallation of 1.9 cm (¾ in) × full width pieces at both ends. Additional laminar cracking in 85/15 ZrO_2/CoCrAlY propagated nearly 100% through specimen. Major radial crack across center of ZrO_2.
3	922°K (1200°F) system; machined	At idle, small laminar crack occurred at one end at 85/15 ZrO_2/CoCrAlY - 40/60 ZrO_2/CoCrAlY interface. Moderate ZrO_2 surface overheating 394°K (250°F) at 6 second accel. Severe laminar cracking at 85/15 ZrO_2/CoCrAlY-ZrO_2 interface at both ends. Crack extends approximately 80% through specimen. No radial cracking evident.
4	922°K (1200°F) system as sprayed; substrate modified for residual stress measurement	Complete delamination and spallation at 6 second accel. Delamination occurred at ZrO_2 - 85/15 ZrO_2/CoCrAlY interface. No radial cracking apparent

TABLE XI

PRINCIPAL STRESS-STRENGTH RATIOS IN CIRCUMFERENTIAL PLANE OF 922°K (1200°F) SPECIMEN

Properties Used	Residual Stress Used	Material	Residual Stress Max/Min	Engine Cycle: Idle Max/Min	Engine Cycle: 6 sec Accel Max/Min	Engine Cycle: SLTO Max/Min	Engine Cycle: 12 sec Decel Max/Min	Rig Cycle: Idle Max/Min	Rig Cycle: 12 sec Accel Max/Min
1) NAS3-19759	None	ZrO_2	0/0	0.69/0.62	1.88/1.42	1.87/0.80	1.75/0.08		
		85/15 Z/M*	0/0	0.55/0.32	0.98/0.61	0.89/0.19	0.69/0.05		
		40/60 Z/M	0/0	0.41/0.08	0.58/0.16	1.37/0.09	0.86/0.01		
2) NAS3-19759	922°K (1200°F)	ZrO_2	1.00/1.11	1.31/1.26	2.38/1.61	1.61/1.42	0.97/0.35	1.22/1.06	2.08/1.97
		85/15 Z/M	0.22/0.46	0.53/0.62	0.88/0.86	0.86/0.33	0.14/0.27	0.45/0.55	0.61/0.60
		40/60 Z/M	0.06/0.20	0.18/0.22	0.32/0.27	0.54/0.16	0.21/0.12	0.19/0.19	0.44/0.22
3) 922°K (1200°F)	922°K (1200°F)	ZrO_2	0.55/0.76	----	1.83/2.00	1.00/1.70	0.44/0.36	0.89/0.81	1.47/2.93
		85/15 Z/M	0.51/0.83	----	1.24/1.07	1.20/0.50	0.60/0.25	0.68/0.62	1.14/0.76
		40/60 Z/M	0.27/0.54	----	0.62/0.76	0.42/0.41	0.23/0.28	0.40/0.51	0.51/0.58

*Z/M = ZrO_2/CoCrAlY